WASHINGTON UNIVERSITY
SEVER INSTITUTE OF TECHNOLOGY

HEAT REGENERATORS WITH PHASE-CHANGE MATERIALS

By

Henry F. Erk

Prepared under the direction of Professor M. P. Duduković

A proposal presented to the Sever Institute of
Washington University in partial fulfillment
of the requirements for the degree of

DOCTOR OF SCIENCE

April, 1990

Saint Louis, Missouri

WASHINGTON UNIVERSITY
SEVER INSTITUTE OF TECHNOLOGY

ABSTRACT

HEAT REGENERATORS WITH PHASE-CHANGE MATERIALS

by Henry F. Erk

ADVISOR: Professor M. P. Duduković

April, 1990

Saint Louis, Missouri

A research project exploring heat recovery and storage in tower regenerators packed with phase-change material is discussed. Such phase-change regenerators (PCRs) could be used in many applications, ranging from storage of solar energy for domestic heating to providing a source of high-temperature blast gas in the metalurgical industries.

A review of conventional heat regenerators, including an equipment survey and survey of mathematical models, is presented. The Stefan problem, *i.e.* the mathematical treatment of phase-change heat conduction and storage, is discussed; solution methods are reviewed. A literature survey of mathematical and experimental research on phase-change heat storage is presented.

The concept of an ideal PCR is introduced and modeled. Thermal efficiency for the ideal case is presented. The mathematical modeling of PCRs is discussed. Equations describing the energy and temperature profiles within a PCR are presented. Equations describing the cyclically operated PCR are presented.

A research plan containing a balanced combination of mathematical modeling and experimentation is presented. Methods for numerically solving the model equations are discussed. An approach for calculating the equilibrium-cycle temperature response for a periodically cycled PCR is outlined. Experiments focused on ascertaining the validity of the models are described.

TABLE OF CONTENTS

LIST OF FIGURES

LIST OF TABLES

1. Introduction

1.1. Motivation

Recently thermal energy users have been compelled to reduce fuel consumption. Two factors are responsible:

- economic — the depletion of nonrenewable, low-cost energy sources results in the conversion to more expensive fuels;
- legislative — the imposition of emission standards for pollutants such as SO_x, NO_x, and CO_x forces reduction in fuels burned.

These two constraints hit energy consumers in the pocketbook: higher fuel costs and higher capital costs for pollution control equipment. The only means of reducing fuel consumption while maintaining capacity is to improve energy utilization efficiency.

As if this were not enough, another constraint is being imposed which encourages energy conservation, *i.e.*

- legislative — the imposition of maximum temperature levels for effluent and exhaust forces additional heat recovery from waste streams.

Gunn [1][†] estimates that approximately eleven percent of the energy consumed in the manufacturing sector is rejected as waste heat. Clearly there is a need to improve waste-heat recovery technology.

There is also great pressure in the private sector to reduce fuel consumption. The energy crises of the seventies, *i.e.* the Arab oil embargo of 1973 and the turmoil in Iran which began in 1978, have underscored the importance of developing alternative energy sources. A large amount of fossil fuel is consumed for

[†]The numbers in braces refer to references in the bibliography.

residential/commercial heating: either directly in the form of burning coal, oil, or natural gas; or indirectly through the use of electricity which is generated from fossil fuel. Hunt [2] estimates that in the United States thirty-seven percent of the total energy demand is for residential/commercial use. Of this percentage fifty-two percent is used for space heating and nine percent is used for water heating. Thus domestic heating accounts for nearly twenty percent of the energy consumed in the United States.

The use of solar energy has long been proposed as an alternative energy source for domestic heating. Unfortunately the cyclic supply of radiant solar energy does not always match the thermal energy demand. Techniques for providing a buffer between the supply and demand are required. One of the most efficient of these techniques is latent heat storage: the thermal energy generated from solar radiation is stored in the reversible phase change of a substance. The concept of latent heat storage for domestic heating applications is almost sixty years old [3], yet this is not utilized extensively today.

Faced with the stark reality of ever-diminishing fossil fuel supplies, and the recognition of all the costs associated with using fossil fuels, it is apparent that there is a need to improve thermal energy storage and recovery technology. Substitution of latent heat for sensible heat in conventional heat storage/recovery equipment is one improvement which could reduce consumption of fossil fuel with virtually no equipment modification.

Consider the fixed-bed heat regenerator, a mainstay of thermal energy storage (TES), where energy is stored in the sensible heat of the packing material. Greater amounts of energy could be stored at near isothermal conditions if the packing were replaced by an encapsulated phase-change material (PCM). The concept of PCM heat storage has been explored for low surface-area-to-volume geometry, *e.g.* pipes filled with PCM. However the rate of heat storage is limited by solid/liquid interfacial area. The heat storage rate per unit volume is low. In this case

increasing the surface area to volume ratio by discretely distributing PCM, *e.g.* filling the regenerator with spheres of PCM, makes sense. This concept has not been extensively explored in the open literature and there is a clear need for modeling and experimental studies to ascertain its effectiveness.

This proposal outlines a course of research conducted to answer salient questions related to the phase-change heat regenerator (PCR). PCRs have applications in industry, for heat conservation and recovery; and in effectively utilizing solar energy for domestic heating applications.

1.2. Objectives

The objectives of this research project center around developing an understanding of how PCRs perform. Specifically, the following items are proposed:

1. Develop a mathematical model for a fixed-bed heat regenerator which utilizes an encapsulated or supported PCM. Investigate the single-blow thermal efficiency as a function of operating parameters and compare results with those predicted for conventional sensible-heat regenerators.
2. Investigate cyclic operation of a PCR. Devise methods for calculating the steady-state or equilibrium cycle. Explore the overall thermal efficiency of this regenerator and compare with a conventional regenerator.
3. Experimentally validate models on a small-scale laboratory regenerator. If discrepancies exist between model and experiment ascertain why and suggest refinements.

The remainder of this proposal is divided into three chapters. The next chapter presents background material and cursory literature reviews. Chapter 3 presents a discussion of preliminary work. The final chapter presents a discussion of the proposed work.

2. Background

This chapter is divided into two sections. The first section reviews conventional heat regenerators describing the advantages and disadvantages of these devices; key parameters and models for regenerators are then presented. The second section begins by presenting a brief review of techniques for solving the Stefan problem, *i.e.* the problem of heat transfer with phase change. The section concludes with a review of the literature on phase-change heat storage.

2.1. Heat Regenerators

Before reviewing pertinent regenerator theory we shall examine the advantages and disadvantages of regenerators relative to other conventional heat recovery equipment.

2.1.1. Equipment Survey

Basically there are two types of heat recovery devices: recuperators and regenerators. Recuperators are heat exchangers; heat is transferred from the waste stream through the wall and then finally into the process stream. Regenerators are heat storage devices as well as heat exchangers; heat is transferred from the waste stream into storage media, and later transferred from the storage media to a process stream. The simplest regenerator is a tower which is packed with high heat-capacity packing. For high temperature applications the packing may be refractory brick arranged in the form of a checkerwork.

Table 2.1 gives a comparison between recuperators and tower regenerators. Regenerators offer high heat transfer areas per unit volume, high heat transfer

Table 2.1

Comparison Between Regenerators and Recuperators‡

Attribute	Regenerator Tower	Recuperator
stores heat	yes	no
heat supply	cyclic	continuous
outlet stream temperature	varying	constant
heat transfer	direct	indirect
ease of turndown	easy	difficult
heat transfer area/volume	high	low
thermal efficiency	medium	high
ease of fabrication	easy	difficult
relative capital cost	low	medium
handling solid laden streams	easy	difficult
subject to fouling	no	yes

‡Comparison based upon information in Reiter [4] and Reay [5]

rates, a wide operating range, and can effectively operate at very high or very low temperatures. A major deficiency of regenerators is the inability to deliver a uniform and continuous supply of heat efficiently.

Regenerators are used in high temperature applications with abrasive (*e.g.* soot laden) streams. For example regenerators are utilized to recover waste heat from flue gas, using the energy to preheat incoming burner air in fired boilers. In these applications the walls of a recuperator would have to be made from exotic alloys or ceramics, formed in complex geometries. With continuous long-term operation the abrasive soot may erode holes into the recuperators walls, degrading performance. On the other hand a tower regenerator is fabricated from the same materials, but built from simple shapes; *e.g.* bricks, spheres, rings, saddles, *etc.* which can be relatively inexpensive to manufacture. Abrasive soot will erode the packing within tower regenerators, but this does not influence the performance.

Regenerators are utilized as a high temperature heat supply for the metalur-

gical and glass-manufacture industries where heat is required in cycles for batch processing. For example, Cowper stoves 50 m tall and 11 m in diameter have been used to supply 500,000 m^3/h of high temperature (1000 to 1300°C) blast gas for iron smelting [6]. The cyclic nature of regenerators compliments the heat requirements for these batch processes. Unfortunately, regenerators do not supply a constant temperature which may be desirable, *e.g.* for heat soaking bricks; some energy is wasted because the regenerator is operated at an average temperature in excess of the required temperature.

Regenerators have been used in place of heat exchangers in gas separation and liquefaction. For this application the packing consists of thin, highly conductive, metal strips which are wound radially within the tower. Here the regenerator acts as a feed air purifier as well [7]. Process vent gas and feed gas alternately flow through the tower. When the cold, expanding vent gas flows through the tower, packing temperature drops to a low temperature as the gas is heated. After several minutes valves redirect the streams so that now the feed gas flows countercurrently through the tower. Water, carbon dioxide, and other condensible gases freeze on the packing while the feed gas is cooled. The feed air is thus purified. Condensibles are flushed out by the vent gas during the next cycle.

Two or more regenerators may be coupled together for continuous energy recovery. In the simplest configuration two units are interconnected via manifolds and valves so that one regenerator is absorbing energy from the hot process stream while the other regenerator is releasing energy to the cold process stream. The time during which the unit stores energy from the hot process fluid is called the heating period, while the time during which the unit releases energy to the cold process stream is called the cooling period. The units are piped so that each regenerator may be cycled, or swung, between heating and cooling periods. For this configuration to be efficient, the length of the heating period should be equal to that of the cooling period. In this case, the two regenerators are alternately

cycled so that one of the two units is in a heating period while the other is in a cooling period.

Two modes of regenerator operation exist in this configuration:

- countercurrent or counterflow, and
- cocurrent or parallel.

Figure 2.1 shows schematics of these two modes. In countercurrent operation the

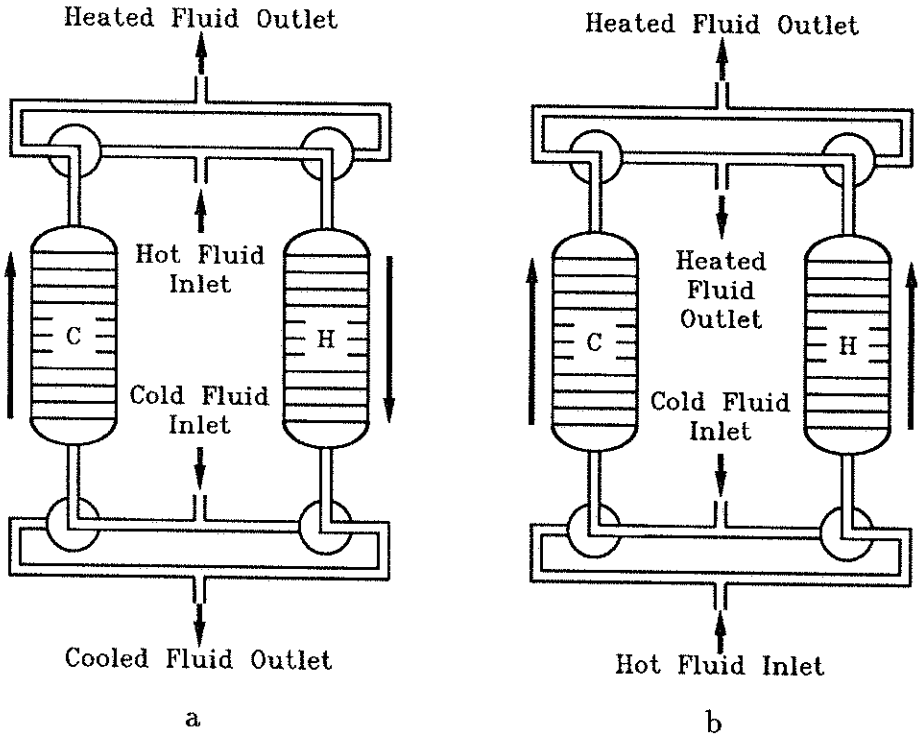

Figure 2.1 Continuous packed-tower regenerators. Fig 2.1.a: countercurrent or counterflow. Fig 2.1.b: cocurrent or parallel flow. The regenerators labeled 'C' are in a cooling period. The regenerators labeled 'H' are in a heating period.

process streams flow in reverse directions through the unit, *i.e.* during the heating period the hot-process stream flows in one direction and during the cooling period the cold-process stream flows in the other direction (*e.g.* in Fig. 2.1.a the hot-process stream flows downward while the cold-process stream flows upward). Four

three-way valves cycle the units through alternating heating and cooling periods. For example in Fig. 2.1.a when the regenerators are to be swung the four valves rotate ninety degrees counterclockwise; the right-hand regenerator swings from heating period into cooling period and the left-hand unit swings from cooling period into heating period.

Flow reversal can be an advantage when one of the process streams is dirty or contains significant amounts of a component which may condense and/or freeze on the packing or checkerwork. In this case channels in the regenerator may become clogged, however, when the flow is reversed the debris is backflushed out of the unit [8].

Analogous to counterflow heat exchangers, counterflow regenerators transfer heat with a more or less uniform gradient throughout the length of the bed. In a heating period hot fluid enters the bed at the warmest end (the top of the bed in Fig. 2.1.a) and exits at the coolest. In a cooling period cold fluid enters at the coolest end and exits at the warmest.

Figure 2.1.b shows the cocurrent mode of regenerator operation. In this mode the hot and cold process streams flow in the same direction through the unit, *e.g.* upward in Fig. 2.1.b. By rotating the four three-way valves ninety degrees counterclockwise the right-hand regenerator swings from heating period to cooling period, while the left-hand regenerator swings from cooling period to heating period. In contrast to countercurrent regenerators, cocurrent regenerators may suffer from plugging when processing dirty streams. Analogous to parallel flow heat exchangers, the temperature gradient in a counterflow regenerator is the greatest at the inlet and the smallest at the outlet.

A variation of the packed tower regenerator is the rotary regenerator: the Ljungstrom [4] or Munter wheel [5] and the Rothemuhle regenerator [4]. Figure 2.2.a shows a schematic of the Ljungstrom wheel. A checkered-matrix wheel rotates at 1–20 rpm. within a split duct. The hot stream flows through one side of

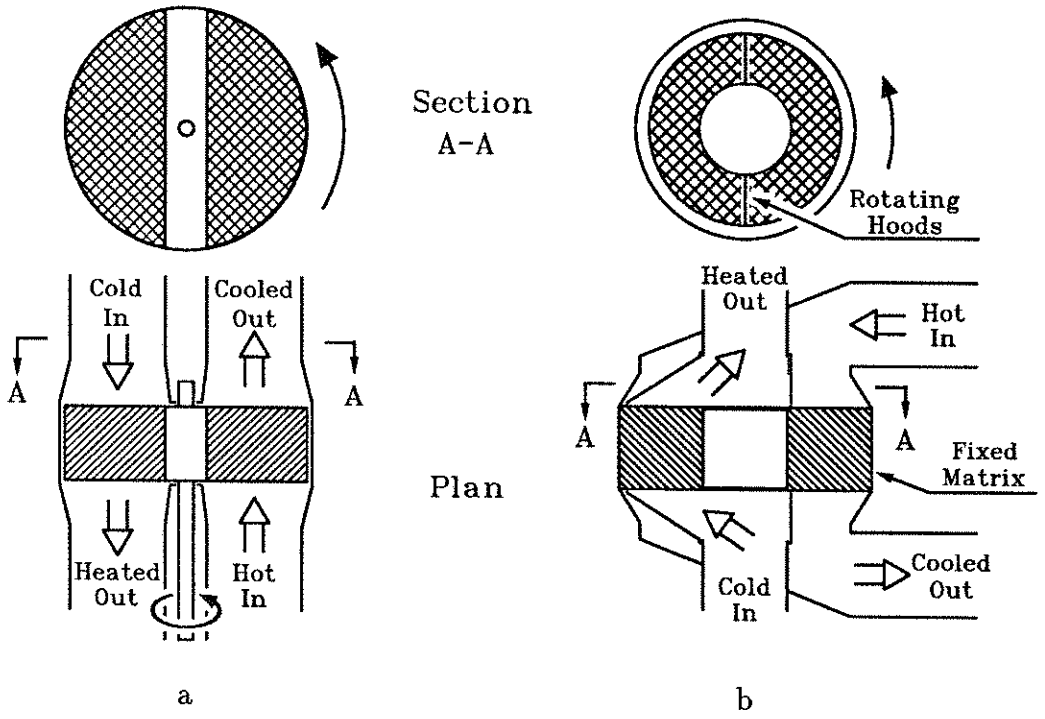

Figure 2.2 Rotary regenerators. Fig. 2.2.a: Ljungstrom regenerator. Fig. 2.2.b: Rothemuhle regenerator. Adapted from [5].

the duct, while the cold flows though the other side. The portion of the matrix in contact with the hot process stream is heated; the absorbed heat is released when this section of the wheel rotates into the cold stream duct. Flexible circumferential seals and face seals minimize cross-stream contamination in low temperature applications. In high temperature applications no seals are used at all. To minimize contamination the pressure difference between the two streams must be limited to approximately 10 kPa. With this limitation contamination is kept to below 0.5 percent for low temperature units and 4 percent for high temperature units. In applications where contamination cannot be tolerated a purge flow may be used. This flow is directed through a duct which lies between the two process ducts. Heat transfer is regulated by varying the rotation speed of the wheel as well as stream flows.

In the Rothemuhle regenerator, Fig. 2.2.b, instead of a rotating wheel inside stationary ducts, there is a stationary matrix with rotating hoods which act as moving ducts. Flexible seals may be used in low temperature applications to minimize contamination.

The rotary regenerator is used in power plants and steam generation facilities to recover heat from burner exhaust gas. In Europe they are also used to pre-condition air temperature and humidity in building heating, ventilation and air conditioning (HVAC) applications. Rotary regenerators offers high heat transfer capacity at relatively low costs. A major drawback with these devices is some cross-stream contamination. [5].

Further information on regenerators can be found in Reay [5], who presents a compendium of regenerator equipment, manufacturers and specifications.

Summarizing our review of heat recovery devices: regenerators have advantages over recuperators in applications where heat demand and/or supply is cyclic or intermittent. Regenerators can be effective in very high or very low temperature applications, especially when process streams are dirty. Despite the fact that regenerators must be cycled, multiple regenerators can be operated to provide continuous heat supply. Continuous regenerators such as the Ljungstrom wheel or the Rothemuhle regenerator are useful in heat recovery applications.

2.1.2. Regenerator Models

Parameters for regenerator operation will now be presented. A review of models for heat regenerators follows.

2.1.2.1. Parameters. Major regenerator parameters are the fluid exit temperature and the thermal efficiency. The regenerator temperature profile may also be of interest. If the regenerator is used for heat recovery, efficiency is the key

parameter. If however the regenerator is used as a heat supply, outlet temperature is the key parameter. In general one of the parameters is optimized at the expense of the other, *e.g.* a regenerator optimized to maximize efficiency may not be effective as a constant-temperature heat supply. Regenerator models are formed from energy balances, so the temperature profile and outlet temperature may be obtained. Thermal efficiency (or effectiveness) is calculated from the outlet temperature history. Efficiency is defined as the ratio of the amount of energy which has been exchanged to the total amount of energy which theoretically could be exchanged.

Consider a single packed-tower heat regenerator at a constant, uniform temperature which is subject to a step-change in inlet fluid temperature. We wish to describe the single-blow (or single-blast) efficiency. Define the following notation:

process fluid inlet temperature (°K)	$T_{i,x}$
process fluid outlet temperature (°K)	$T_{o,x}$
process fluid heat capacity (J/kg °K)	$C_{p,x}$
process fluid mass flowrate (kg/s)	$\dot{m}_x$
period duration (s)	θ_x
energy stored during period (J)	Q_x
period efficiency (·)	η_x
the running time coordinate (s)	τ

where the subscript x is replaced by h for a hot blast and by c for the cold blast. Figure 2.3 shows how the outlet fluid temperature varies between $T_{i,h}$ and $T_{i,c}$ over several heating and cooling periods for this typical regenerator.

In calculating single-blow thermal efficiencies one assumes that at the end of the period the regenerator packing is in thermal equilibrium with process fluid.

During any blast the total amount of heat which is absorbed by the packing, Q_x, is the total change in the sensible heat of the process fluid; *viz.*:

$$Q_x = \pm \dot{m}_x C_{p,x} \int_0^{\theta_x} (T_{i,x} - T_{o,x})\, d\tau \tag{2.1}$$

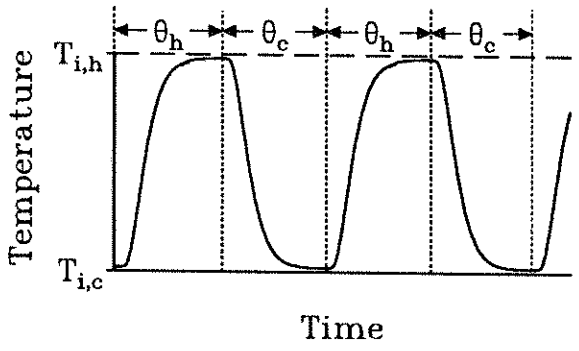

Figure 2.3 Typical regenerator outlet-fluid temperature history.

where for a hot blast $x \rightarrow h$ and the $+$ sign in front of the integral applies; for a cold blast $x \rightarrow c$ and the $-$ sign applies. The ideal, thermodynamics-limited, amount of heat which the regenerator can store, Q_x^{id}, is given by the energy difference between the hot-process fluid and the cold-process fluid, *viz.*:

$$Q_x^{id} = \dot{m}_x \, C_{p,x} \, \theta_x \, (T_{i,h} - T_{i,c}) \tag{2.2}$$

The preceding two equations are based upon the assumptions that $\dot{m}_x$ and $C_{p,x}$ are constant or are overall integral-averaged values.

The single-blow thermal efficiency is

$$\eta_x \equiv \frac{Q_x}{Q_x^{id}} \tag{2.3}$$

On substituting eq. 2.1 and eq. 2.2 into eq. 2.3 and simplifying, one obtains

$$\eta_x = \frac{\pm \int_0^{\theta_x} (T_{i,x} - T_{o,x}) \, d\tau}{\theta_x \, (T_{i,h} - T_{i,c})} \tag{2.4}$$

Equation 2.4 may be further simplified if one changes the temperature scale. Define a dimensionless temperature scale by

$$t = \frac{(T_{i,h} - T)}{(T_{i,h} - T_{i,c})} \tag{2.5}$$

e.g. $t_{o,h}$ is the dimensionless temperature for $T = T_{o,h}$. This scaling maps the actual temperature range onto the interval $[0, 1]$. Now for a hot blast eq. 2.4 becomes

$$\eta_h = \frac{\int_0^{\theta_h} (1 - t_{o,h})\, d\tau}{\theta_h} \tag{2.6}$$

The hot-period single-blow thermal efficiency is given by dividing the area above the thermal **F** curve by the length of the period. This curve is the dimensionless response to a step-up change in inlet conditions. Levenspiel [9] has defined the **F** curve in terms of concentration, here temperature is substituted. Figure 2.4 shows a typical **F** curve for a hot blast. When a regenerator operates at high

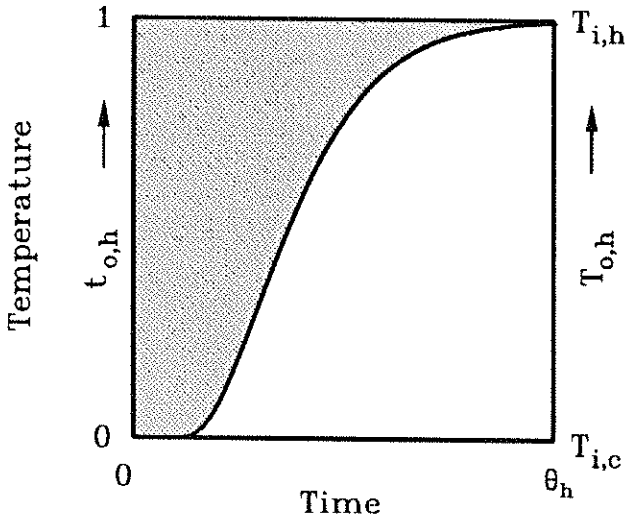

The shaded area is given by the integral:

$$\int_0^{\theta_h} (1 - t_{o,h})\, d\tau \; .$$

Larger shaded areas indicate higher efficiencies. Here the efficiency is approximately 0.44.

Figure 2.4 Typical **F** curve for a regenerator in a heating period.

efficiency the area above the curve will be large, *i.e.* $t_{o,h}$ will be close to zero, indicating a large fraction of the energy available in the process fluid has been stored in the unit.

For a cold blast eq. 2.4, simplified in terms of the dimensionless temperature, is

$$\eta_c = \frac{\int_0^{\theta_c} t_{o,c}\, d\tau}{\theta_c} \tag{2.7}$$

In this case the efficiency is given by the area under the **W** curve divided by the length of the period. The **W** curve is the dimensionless response to a step-down change in inlet conditions. For this linear system **W** = **1-F**.

Figure 2.5 shows a typical **W** curve for a regenerator in a cooling period. In

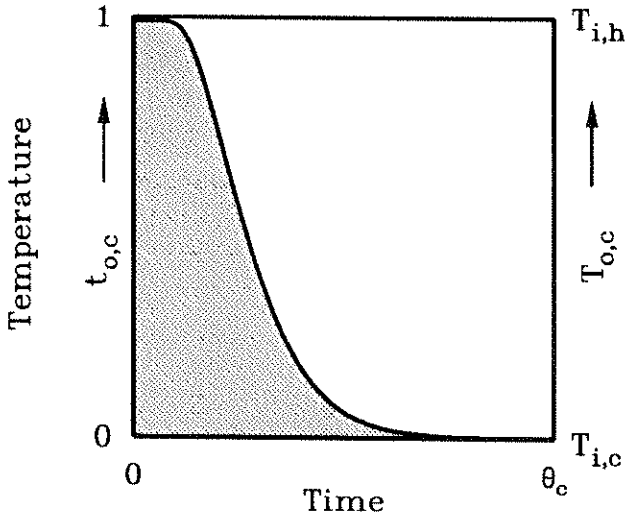

The shaded area is given by the integral:

$$\int_0^{\theta_h} t_{o,c}\, d\tau \ .$$

Larger shaded areas indicate higher efficiencies. Here the efficiency is approximately 0.29.

Figure 2.5 Typical **W** curve for a regenerator in a cooling period.

the cooling period, when a regenerator is operating at high efficiency, the area below the curve will be large, *i.e.* $t_{o,c}$ will be close to one. This indicates that a large fraction of the energy has been transferred to the cold process fluid.

In practice the regenerator period is not long enough to assure thermal equilibrium between the process fluid and the packing. Regenerators are swung at or before thermal breakthrough. In this case the packing temperature is not uniform; efficiency is not given by the single-blow value. The overall efficiency of the regenerator, η^o is defined:

$$\eta^o \equiv \frac{Q_h + Q_c}{Q_h^{id} + Q_c^{id}} \tag{2.8}$$

The definition of η^o parallels that of the single-blow efficiencies, although strictly speaking the responses are no longer **F** and **W** curves.

2.1.2.2. Models. The classical mathematical treatment of regenerators has been summarized by Jakob [10], Hausen [6], and Schmidt and Willmott [8]. Models for single blow operation can be written for six ideal cases:

1. The regenerator periods are essentially zero and the regenerator is cycled infinitely fast.
2. The packing thermal conductivity is infinite.
3. The packing thermal conductivity is infinite along the regenerator axis and finite along the cross section.
4. The packing thermal conductivity is zero along the axis and infinite along the cross section.
5. The packing thermal conductivity is zero along the axis and finite along the cross section.
6. The packing thermal conductivity is finite along the axis and zero along the cross section.

Cases 1 and 2 are not realistic. Case 3 is applicable only for short regenerators with heavily insulated walls; one of limited use. Case 4 describes low-temperature regenerators used in gas liquefaction. Cases 5 and 6 describe high-temperature regenerators used in metalurgical and glass industries. Either case 5 or 6 can describe a regenerator which contains a checkerwork or random packing.

Nusselt [11] discussed the first five cases. He considered only convective-film heat transfer and neglected temperature gradients within the packing. This simplifying assumption was also used by Anzelius [12], Hausen (described in [6]), and Schumann [13] who each independently presented solutions of case 4. The simplified model of case 4 is often referred to as the Schumann model. Klinkenberg [14] has reviewed both numerical and analytic solutions for the Schumann model. Larsen [15] presents a numerical approximation.

Nusselt [11] described an approximate solution method using a finite difference scheme for the case 5. Handley and Heggs [16] present a numerical solution for a packed bed, under the conditions of case 5 including the effects of intraparticle

conduction and film convection. Schmidt and Szego [17] describe a finite-elements solution for regenerator channels also including these effects.

Case 6 has been solved numerically by Burch *et al.* [18] using finite differences and Lu [20] who numerically inverted the Laplace-transform analytical solution. Both Burch *et al.* and Lu assumed that heat transport due to fluid flow is negligible. Lai [19] presents and approximate solution for case 6 as a function of the mean and variance of the impulse response.

All the preceding models have considered single-blow operation. To predict the overall efficiency and performance of a swing regenerator it is necessary to calculate the equilibrium cycle. Here a cycle is defined as a hot blow followed by a cold blow.

The analysis of the periodic cycling of regenerators follows two different approaches: the closed method and the open method. To apply the closed method a closed-form solution, either exact or approximate, is obtained for the model equations; *e.g.* cases 1 through 6, for one cycle. This solution is a function of the initial condition (IC), *i.e.* the temperature profile within the regenerator; thus the solution for a given cycle depends upon the solution of the previous cycle. Cyclic equilibrium requires that the solution for one cycle is equal to the solution for the next. Equating two successive cycles allows one to find this.

To apply the open method a model is evaluated for a cycle. At the end of the cycle the current conditions are used as the IC for the next cycle and the model is solved again. This process iterates until repeatable cycles evolve. The model is cycled just as the regenerator. Assuming the model is not chaotic, the equilibrium cycle is reached.

Nusselt [11] described a closed method analysis for a countercurrent regenerator modeled as case 4. Ackermann [21] extended the analysis and found the solution in terms of a Fourier series and another series which was obtained by

application of Volterra integral equations. Nahavandi and Weinstein [22] also present a closed-method solution, using an infinite series representation of the solution's IC and solving for the constants of this series.

Hausen [6] reviews equilibrium cycle calculations. He describes a complex closed method analysis using eigenfunctions for cocurrent and countercurrent regenerators described by case 4. Kardas [23] has performed a closed-method analysis for cocurrent regenerators described by case 5. Lai [19] performed closed-method analyses for packed bed regenerators (case 6) for both cocurrent and countercurrent operation.

The work of Willmott [24] is a typical application of the open method. Willmott simulated a regenerator described by case 4 using a finite difference scheme. He started the computation with an IC which he hoped approximated that of the equilibrium cycle and began the simulation. After several simulated cycles the calculations converged.

All the models considered here are linear and techniques such as superposition can be applied to establish the equilibrium cycle. Unfortunately, when one considers phase-change heat storage the model is no longer linear.

This completes the review of heat regenerators. The next section presents a review of phase-change heat transfer.

2.2. Phase-Change Heat Storage

The mathematical description for transient heat transfer with a phase change is called the Stefan problem in honor of J. Stefan who studied this problem in the 1890's. A review of methods for solution of this problem is now presented. A review of phase-change heat transfer follows.

2.2.1. Stefan Problem Solution Techniques

Consider a PCR filled with spherical PCM. Assume the PCM is composed of two components: a matrix of inert material (support component) filled with a heat storage substance (phase-change component). Both components have finite heat capacity and thermal conductivity. The equations which follow are valid for a heating period where the PCM changes from solid to liquid. A similar analysis can be performed for the cooling period but is not presented here. Define the following terms:

y-phase temperature (°K)	T_y
PC melting temperature (°K)	T_M
fluid temperature around PCM sphere (°K)	T_f
z-component density (kg/m^3)	ρ_z
z-component heat capacity (J/kg °K)	$C_{p,z}$
z-component thermal conductivity (W/m °K)	k_z
convective transfer coefficient (W/m^2 °K)	h_B
PC latent heat of fusion (J/kg)	λ
spatial coordinate — radius (m)	r
PCM sphere radius (m)	R_{PCM}
PCM support porosity (m^3 PC/m^3 PCM)	ϵ_{SC}
SC tortuosity (m pore/m radius)	τ_{SC}

where the subscript y is replaced by l to designate liquid phase and s to designate solid phase, and the subscript z is replaced by sc to designate support component and pc to designate phase-change component. Assuming the physical properties of the phase-change component are constant and equal for both phases, the effective PCM properties are

$$\rho_{PCM} = \rho_{PC}\,\epsilon_{SC} + \rho_{SC}\,(1-\epsilon_{SC})$$

$$C_{p,PCM} = \frac{C_{p,PC}\,\rho_{PC}\,\epsilon_{SC} + C_{p,SC}\,\rho_{SC}\,(1-\epsilon_{SC})}{\rho_{PCM}}$$

$$k_{PCM} = \frac{1}{\tau_{SC}}\left[k_{PC}\,\epsilon_{SC} + k_{SC}\,(1-\epsilon_{SC})\right]$$

The expression for k_{PCM} assumes that the matrix tortuosity is equal to the pore tortuosity. This assumption is valid for an open-pore structure with uniform-thickness walls and narrow pore-size distribution.

The energy balance for each phase is the classical Fourier equation:

$$C_{p,PCM}\,\rho_{PCM}\,\frac{\partial T_y}{\partial \tau} = k_{PCM}\,\frac{1}{r^2}\,\frac{\partial}{\partial r}\left(r^2\frac{\partial T_y}{\partial r}\right) \quad \begin{cases} 0 < r < \delta & y = s \\ \delta < r < R_{PCM} & y = l \end{cases} \tag{2.9}$$

Equation 2.9 is based upon the assumptions that physical properties are constant and equal for both phases, and that there is no liquid-phase convection. To incorporate convection one must augment the energy equation with a momentum-balance equation, *e.g.* the Navier-Stokes equation.

The position of the solid/liquid interface, δ, is given by a heat flux balance:

$$k_{PCM}\,\frac{\partial T_s}{\partial r} - k_{PCM}\,\frac{\partial T_l}{\partial r} = \lambda\,\rho_{PC}\,\epsilon_{SC}\,\frac{d\,\delta}{d\,\tau}\,; \qquad r = \delta \tag{2.10}$$

If solid and liquid densities are not equal, a convective term must be added to eqs. 2.9 and 2.10. Equation 2.10 is valid when the support conductivity is of the same order of magnitude as (or less than) the conductivity of the phase-change component. If the support conductivity is much greater than the conductivity of the phase-change compound, heat is conducted by the matrix throughout the entire sphere faster than it is consumed by phase change. A flat temperature profile develops within the sphere. The solid/liquid interface is parallel to the pore walls of the matrix. The mathematical description of this interface is very complex and cannot be described by eq. 2.10

When eqs. 2.9 and 2.10 are applicable the boundary conditions (BCs) are:

$$r = 0\,; \qquad k_{PCM}\frac{\partial T_s}{\partial r} = 0 \tag{2.11.a}$$

$$r = \delta\,; \qquad T_s = T_l = T_M \tag{2.11.b}$$

$$r = R_{PCM}\,; \qquad k_{PCM}\frac{\partial T_l}{\partial r} = h_B\,(T_f - T_l) \tag{2.11.c}$$

The IC is:

$$\tau = 0\ ; \qquad 0 \leq r \leq R_{PCM}\ ; \qquad T_s(r) = T^i(r) \tag{2.12}$$

where $T^i(r)$ represents the initial temperature profile in the PCM.

Because this problem consists of two coupled partial differential equations (PDEs) with a moving boundary, an analytical solution on the finite domain exists only for simple cases [25]. The analytical solution of Neumann [25] applies for the semi-infinite slab. Crank [26] describes other solutions.

Reviews by Muehlbauer and Sunderland [27], and Mori and Araki [28] do not present analytical solutions for spherical geometry with the BCs given above. To the best knowledge of this author, an analytical solution for this problem has not been reported.

Approximate methods for solving the Stefan problem may be grouped into two categories: front-tracking and fixed-domain. In front-tracking methods eq. 2.10 is solved along with the (PDEs) represented by eq. 2.9. Numerical methods such as finite differences, finite elements, orthogonal collocation, collocation on finite elements, *etc.* are employed to discretize either the spatial or temporal coordinate; or both. For example, Furzeland [29] discusses methods which discretize in time or space using finite differences. Schneider and Raw [30] describe the application of finite differences in space. Chawla *et al.* [31] present a spatial collocation method in which the collocation points move with the melt interface. In some instances the solid/liquid interface is immobilized (dividing r by δ), however this cannot be considered a fixed-domain method because δ must still be computed via the flux balance, eq. 2.10.

In fixed-domain methods the energy balance is treated differently. The latent heat is introduced into the energy balance as an enthalpy term or as a modified heat capacity. The most frequently used technique for implementing this method is to invoke an enthalpy function, U which is

$$U(T) = \int_{T_{i,c}}^{T} C_{p,PCM}(T)\, dT \; + \; \chi\, \lambda\, \epsilon_{SC} \tag{2.13}$$

where

$$\begin{aligned} &\text{for} \quad T_y < T_M \qquad \chi = 0 \\ &\text{for} \quad T_y = T_M \qquad 0 \le \chi \le 1 \\ &\text{for} \quad T_y > T_M \qquad \chi = 1 \end{aligned}$$

The contribution to the energy balance due to latent heat of fusion is taken up in a change in enthalpy. Since the phase change occurs at T_M the enthalpy function automatically brings latent heat into the conduction equation, which becomes

$$\rho_{PCM} \frac{\partial U}{\partial \tau} = k_{PCM} \frac{1}{r^2} \frac{\partial}{\partial r} \left(r^2 \frac{\partial T_{PCM}}{\partial r} \right) \; ; \qquad 0 < r < R_{PCM} \tag{2.14}$$

where T_y is replaced by T_{PCM} to emphasize that there is only a single PDE to be solved. Note that eq. 2.13 *cannot* be substituted into eq. 2.14 since differentiation of χ would give a Dirac delta function at the τ where $T_{PCM} = T_M$. Equation 2.14 must be solved together with eq. 2.13. The BCs are given by eqs. 2.11.a and 2.11.c with the subscripts s and l on T replaced by PCM. The IC is given by eq. 2.12 (with s replaced by PCM) or

$$\tau = 0 \; ; \qquad 0 \le r \le R_{PCM} \; ; \qquad U(r) = U^i(r) \tag{2.15}$$

where $U^i(r)$ represents the initial enthalpy profile.

Shamsundar and Sparrow [32] have discussed implementation of this method. Furzeland [29] and Schneider and Raw [30] have presented numerical examples of the enthalpy method implementation as well. Furzeland [29] reports that front-tracking methods are more accurate than the enthalpy method. In instances where the phase-change front geometry is complex, *e.g.* a highly conductive support matrix, front-tracking methods may be impossible to implement.

In summary: an analytical solution for the Stefan problem under the conditions applicable in a PCR has not been reported. An approximate solution or a numerical solution must be used. In terms of a numerical solution both the front-tracking and fixed-domain methods can be useful. Front-tracking methods may be slightly more accurate. Front-tracking methods cannot be used when the support-matrix conductivity is much greater than that of the phase-change component. Fixed-domain methods are simpler to implement and account for both sensible and latent heat storage in one equation.

2.2.2. Phase-Change Heat Storage Survey

Heat storage using PCM contained in tubes has been extensively explored. In fact a 6 foot long, $3\frac{1}{2}$ inch diameter polyethylene tube filled with Thermal 81® (a stabilized $CaCl_2$ manufactured by Dow Chemical — m.p. of 29.7 °C) which is sealed on both ends is a commercially available product for solar energy storage applications [33].

Katayama *et al.* [34] reported experiments using high aspect ratio tubes filled with naphthalene ($C_{10}H_8$). Experimental results were compared with a front-tracking model which is solved numerically *via.* using an implicit finite difference scheme. The model underpredicted heat storage rate. It was concluded that convection strongly influences heat transfer.

Rieger *et al.* [35] have presented a numerical and experimental investigation of phase-change heat storage in low aspect ratio tubes. Their model includes convective effects, but assumes the solid phase remains fixed in the center of the tube. Model predictions were matched to experiments, using n-octadecane ($C_{18}H_{38}$) as the phase-change material. The model did not properly describe heat transfer in the bottom section of the tube: the solid phase sank to the bottom of the tube (due to density differences between phases) and this effect was not included in the model.

El-Masry [36] presents a model based upon the front-tracking method which includes convection and melt buoyancy effects. He compares model predictions with the data presented by Katayama *et al.* [34] and Rieger *et al.* [35]. Model predictions match the experiments well. El-Masry's model reveals that melt convection can increase heat transfer rates by as much as a factor of two.

Mulligan [37] has described a phase-change heat-storage module for load-leveling of heating utilities in orbiting spacecraft. Heat is stored in a slurry of microencapsulated wax spheres. Eicosane and octadecane spheres with a diameter of 50–100 μm were fabricated with a polymer outer shell for the slurry [38]. There are no public-domain references available on modeling this system.

Phase-change heat transfer within a spherical enclosure have been investigated by Moore and Bayazitoglu [39]. Transparent glass spheres (approximately 3.3 and 2.8 cm diameter) were filled with n-octadecane wax. Visual observations of the melt front could be made. A front-tracking model was written which included convection and solid/liquid phase buoyancy effects. These effects were significant, increasing the heat transfer rates by as much as thirty percent.

Models for a channel-type phase-change heat regenerator were presented by Morrison and Abdel-Khalik [40]. They used the enthalpy method to account for phase-change heat storage. Four models were presented:

1. Case 5 with PCM.
2. Zero thermal conductivity for the PCM and fluid in all directions and zero fluid heat capacity.
3. Model 2 with no convective heat transfer resistance to the channel walls.
4. Model 3 except fluid heat capacity is not zero.

Models 1 and 4 apply when the fluid is a liquid; models 2 and 3 apply when the fluid is a gas. Using the parameters specified in [40] model 4 is a good approximation of model 1 and model 3 is a good approximation of model 2.

A method of storing high-grade heat (approximately 1000 °C) was proposed in [41]. This concept is illustrated in Figure 2.6. The phase-change material is cycled between two towers as a liquid or solid shot. In a shot tower heat is

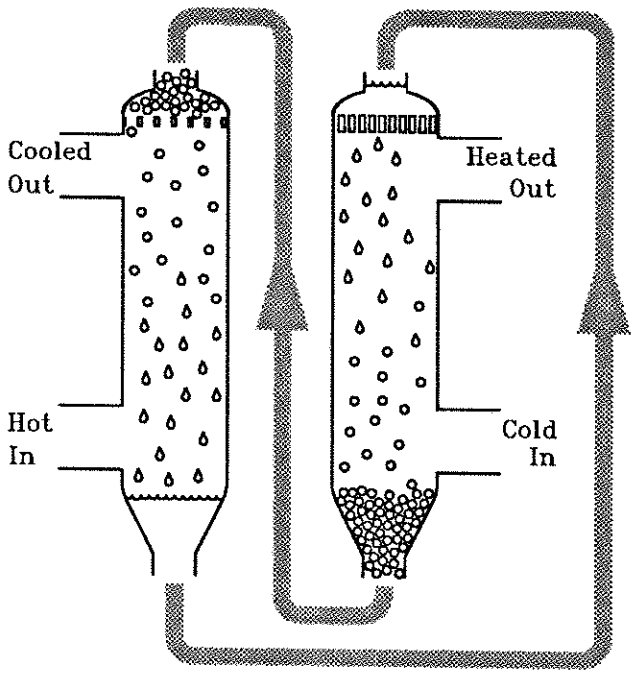

Figure 2.6 High-temperature phase-change heat storage concept.

released to the cold process gas; the molten shot solidifies. The shot are then transferred to another tower where they are contacted with the hot process gas; the shot melts, absorbing heat. The liquid is then recycled to the shot tower. The advantage of this process is that heat transfer is continuous. Major disadvantages include moving solids, pumping high-temperature liquids. This also requires a large process volume.

Olszewski [42] proposed methods for producing encapsulated and supported PCM which could be used in a high-temperature PCR. One concept was a self-encapsulating PCM which is produced by solidifying a silicon-aluminum alloy in a shot tower. During controlled solidification a silicon-rich shell forms around

the aluminum-rich molten core. Since there are opposing Si and Al concentration gradients, the melting point of the alloy decreases moving to the center. Within a temperature range the central core can be melted while the outer shell remains solid. Another concept proposed in [42] is the use of high porosity bricks which are filled with high melting-temperature PCM; the liquid phase is retained by capillary forces.

Arimilli [43] presented calculations for a spherical PCM which is composed of a porous matrix filled with a phase-change alloy. He reports the results for only one case: heat recovery from combustion gases. Unfortunately he does not describe how the calculations were performed, nor does he present details of how phase change was modeled. Adebiyi [44] presents a model for cylindrical PCM in a PCR. His model consists of an equation describing energy transport by fluid convection in the bed. Phase change in the PCM-cylinders, which are treated as spheres of an equivalent diameter, is modeled using the enthalpy method. A few results are presented for a specific application: heat storage in the manufacture of bricks. No other references to PCR models or experiments have been found.

A review of the literature has indicated that no one has systematically and thoroughly quantified all the processes which occur in a PCR. There has been no experimental verification of PCR models. Thus, there is a need to develop a methodology for predicting PCR performance in single-blow and cyclic operation and to experimentally verify the methods developed.

3. Preliminary Work

In accordance with the first objective of this research project a model for a phase-change regenerator needs to be formulated. Before developing the equations an idealized model will be explored.

3.1. Ideal PCR

Consider the ideal regenerator. The characteristic times for all heat transfer and storage processes are much smaller that the characteristic time for temperature convection by bulk flow. Figure 3.1 shows the outlet temperature history for both the ideal sensible-heat regenerator and the ideal PCR. In this figure $\mu_{s,x}$ and $\mu_{l,x}$ ($x = c$ or h) are the thermal break-through times . The subscript s designates sensible heat storage and l designates latent heat storage. These times are a measure of the heat storage capacity.

Define the nomenclature:

PCR tower length (m)	L
process fluid superficial velocity (m/s)	v_f
y phase density (kg/m^3)	ρ_y
y phase heat capacity (J/kg °K)	$C_{p,y}$
porosity of regenerator bed (m^3/m^3)	ϵ_B
accumulation parameter (·)	ψ
Stefan number (·)	Ste

where the subscript y is replaced by f for fluid properties, p or PCM for the regenerator packing (p for sensible-heat storage packing and PCM for phase-change material packing). The two dimensionless groups, Ste and ψ are defined as

$$\psi = \frac{\epsilon_B \, \rho_f \, C_{p,f}}{(1-\epsilon_B) \, \rho_p \, C_{p,p}} \qquad Ste = \frac{C_{p,PCM} \, (T_{i,h} - T_{i,c})}{\lambda \, \epsilon_{SC}}$$

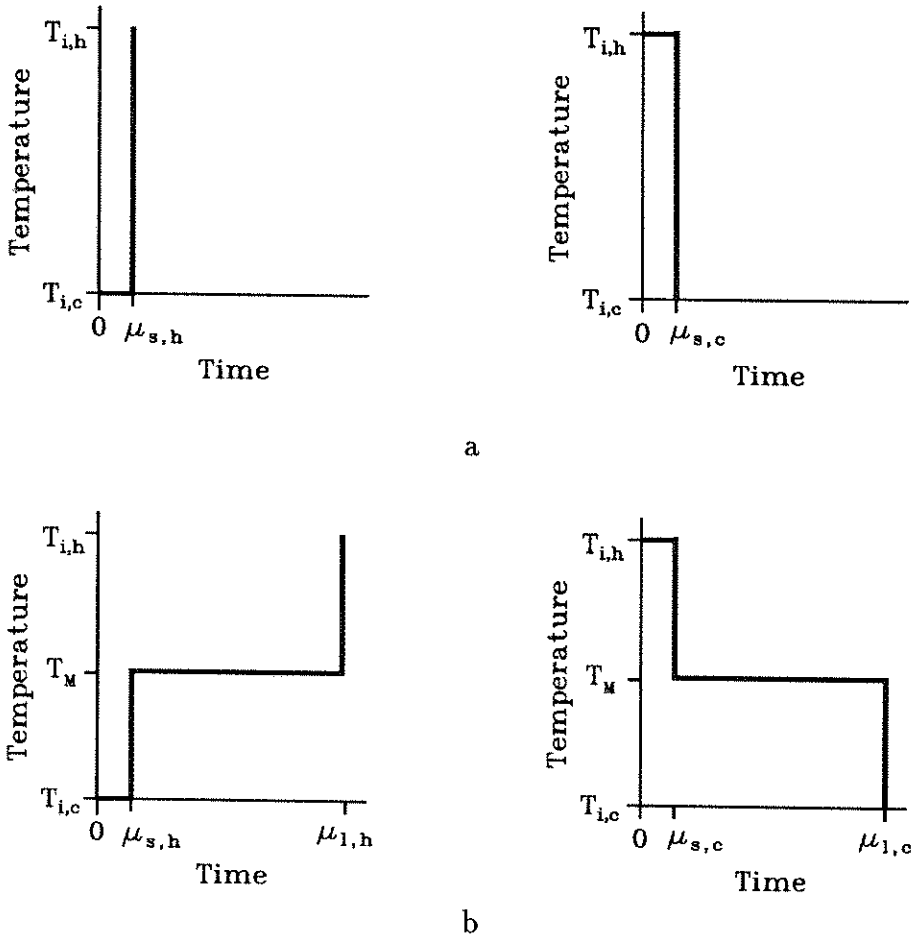

Figure 3.1 Ideal regenerator temperature histories. Fig 3.1.a : ideal sensible-heat regenerator. Fig 3.1.b : ideal PCR. Note $\mu_{s,h}$ and $\mu_{s,c}$ are the same for both figures. In each figure the left plot represents a heating period and right plot represents a cooling period.

The Stefan number, Ste, is the ratio of sensible heat to latent heat. When $Ste \rightarrow \infty$ sensible heat storage dominates, while when $Ste \rightarrow 0$ latent heat storage dominates. The accumulation parameter, ψ, is the ratio of the sensible heat of the fluid to that of the packing. When the fluid is a gas $\psi \rightarrow 0$, when the fluid is a liquid ψ is $\mathcal{O}(1)$.

The break-through times are given by:

$$\mu_{s,x} = (1+\psi)\frac{L\,\rho_p\,C_{p,p}}{v_f\,\rho_f\,C_{p,f}} \tag{3.1}$$

and

$$\mu_{l,h} = \mu_{s,x}\left[1+\frac{1}{Ste\,(1-t_M)(1+\psi)}\right] \tag{3.2.a}$$

$$\mu_{l,c} = \mu_{s,x}\left[1+\frac{1}{Ste\;t_M\,(1+\psi)}\right] \tag{3.2.b}$$

where t_M is the dimensionless temperature defined by eq. 2.5. Equations 3.2.a and 3.2.b indicate the capacity of a PCR is enhanced relative to that of a conventional unit. For a given capacity the volume occupied by a PCR is much smaller than that occupied by a conventional regenerator. A smaller unit is less expensive to build. For example, the volume required to store solar thermal energy in domestic heating applications using sensible heat may be prohibitively large. Using latent heat storage (with $Ste << 1$) the volume can be reduced to a manageable size. In high temperature applications (such a metalurgical, glass, brick, and chemical processing) a conventional regenerator which has been converted to a PCR, simply by replacing the packing with PCM, could be operated for much longer periods before being swung. The service life of the high-temperature switching valves could be increased substantially, reducing maintenance and downtime.

From Fig. 3.1 and using eqs. 2.6 and 2.7 one may derive the ideal single-blow efficiencies:

$$\eta_h = \frac{(1-t_M)\,[Ste\,(1+\psi)\;+\;1]}{Ste\,(1+\psi)\,(1-t_M)\;+\;1} \tag{3.3.a}$$

$$\eta_c = \frac{t_M\;[Ste\,(1+\psi)+1]}{Ste\;\;t_M\,(1+\psi)\;+\;1} \tag{3.3.b}$$

When $Ste \rightarrow \infty$, *i. e.* pure sensible heat storage, the efficiencies approach unity. When $Ste \rightarrow 0$, *i. e.* pure latent heat storage, the efficiencies are

$$\eta_h = 1 - t_M \tag{3.4.a}$$

$$\eta_c = t_M \tag{3.4.b}$$

PCR single-blow efficiencies are less than those for the ideal sensible-heat storage regenerator. Based upon this comparison one may argue that PCRs are not an effective means of reducing energy consumption. However three points must be noted. First, the actual efficiency of conventional regenerators is never one; the efficiency can be as low as 0.65 [5]. Real regenerators are never ideal, nor or they operated in single-blow mode. Second, since PCRs can store more heat per unit volume they may be used in applications where today heat is not recovered. For example, solar energy storage is not implemented because of the prohibitively large volumes required for sensible heat storage. PCRs however may make heat storage viable, saving energy which would not be utilized. Third, PCRs can provide an isothermal heat supply which is required in certain processes. Regenerators may be used instead of recuperators for the reasons discussed in Chapter 2, *e.g.* high-temperature, dirty process streams. Here PCRs can supply heat at a constant temperature which *is* the target process temperature. With conventional regenerators the lowest supply temperature must be near the target temperature, so the unit must be operated at an average temperature *higher* than the target temperature, requiring extra energy. This is illustrated in Figure 3.1. Here regenerators are used to supply process heat rather than to recover heat. Below a certain temperature the energy is useless with respect to the process. In this situation other heat recovery devices and heat integration must be used in conjunction with PCRs to improve the thermal efficiency of the overall plant rather than the specific process.

Consider the ideal PCR as a constant-temperature gas supply. Further, we

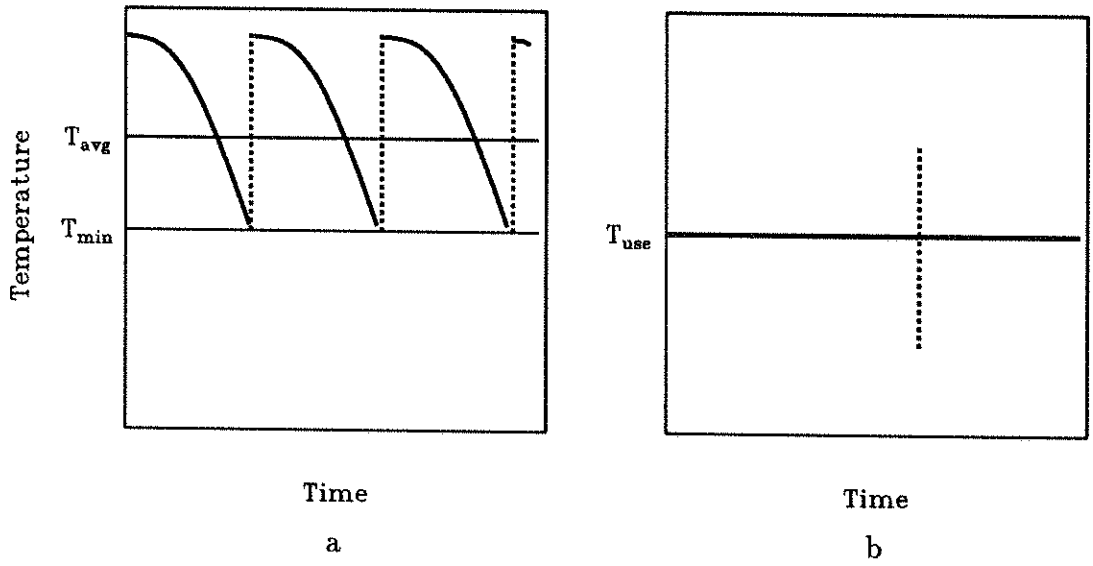

Figure 3.2 Energy savings using PCR regenerators. Fig 3.1.a : temperature history of a sensible-heat regenerator used as a constant-temperature heat supply. Fig 3.1.b : temperature history of a PCR used as a constant-temperature heat supply. $T_{use} = T_{min} = T_M$ for this process. The dashed lines in both figures indicates a swing to another regenerator.

assume Ste is zero, *i.e.* pure latent heat storage. Physical properties are assumed to be constant, and both process streams are flowing at the same rate. The amount of energy retained by the regenerator during a heating period must be equal to the amount of energy released by the regenerator during a cooling period, *viz.*

$$\theta_h \eta_h = \theta_c \eta_c \tag{3.5}$$

Normally one would want to have $\theta_h = \theta_c$. In this case the regenerator is balanced and two regenerators can be cycled as illustrated in Figure 2.1. Thus the regenerator must operate with a t_M of 0.5. Unfortunately this is not always possible nor desirable. When $t_M \neq 0.5$ the regenerator is unbalanced. A *modus operandi* for managing continuous processing must be established.

Borrowing a technique used with conventional regenerators, one may still ef-

fectively operate unbalanced regenerators. The two periods are selected so that one is an integer multiple, κ, of the other; *vis-à-vis* $\theta_h = \kappa\theta_c$ or $\theta_c = \kappa\theta_h$. In this case $\kappa + 1$ regenerators can be connected together to provide continuous processing. Assuming equal v_f for both streams, κ is

$$\left.\begin{aligned} \kappa &= \frac{(1 - t_M)}{t_M} \qquad t_M < 0.5 \\ \kappa &= \frac{t_M}{(1 - t_M)} \qquad t_M > 0.5 \end{aligned}\right\} \tag{3.6}$$

For example, for $t_M = 0.25$ $(\kappa = 3)$ one may use 4 regenerators: one in a heating period, θ_h, and three in a cooling period, $\theta_c = 3\theta_h$. Each of the three regenerators is offset in time from the others by an integer multiple of θ_h, *i.e.* at time τ the first of the three has been operating for τ, the second for $\tau + \theta_h$, the third for $\tau + 2\theta_h$. When the regenerator in the heating period is swung one of the other regenerators is ready to take its place.

This analysis indicates that efficient operation of PCRs will require multiple units which must be properly scheduled. Importance is placed on developing a methodology which can predict θ_x.

3.2. Real PCR

Four heat transfer processes exist in the PCR:

1. Heat convection by fluid flow
2. Dispersion of heat by fluid conduction.
3. Heat convection through the film (thermal boundary layer) surrounding the PCM.
4. Heat conduction/convection in the PCM.

In an ideal PCR the first process is so slow that it alone regulates overall heat transfer. Processes 2–4 reach equilibrium since their heat transfer rates are much greater than the overall rate which is set by process 1. Thus the thermodynamic-limited amount of heat, Q_x^{id}, can be transferred and $\eta_x = 1$.

For a real PCR the first process may not necessarily control the overall rate. For example, a high thermal conductivity fluid will carry energy from the inlet to the outlet of the PCR without allowing it to be stored in the PCR. Poor heat transmission to the PCM, or within the PCM, will reduce the rate of heat storage so that more heat is carried out.

The temperature history may be altered dramatically if one or more of the resistances in processes 2 to 4 dominates. To calculate the correct history the effect of all these processes must be incorporated in a detailed mathematical model. Upon an examination of the solutions from this model one may be able to develop a simpler treatment for PCRs. A major step in this direction is developing a model.

3.3. PCR Model Equations

Consider a PCR which is composed of a tower packed with uniform, spherical PCM. To model this one must account for events which occur on two scales: the tower or bed scale, and the PCM-sphere scale. Two interfaces must be accounted for: the process-fluid/PCM (intraparticle) and the solid-PCM/liquid-PCM (inter-particle). The following assumptions will be made:

1. No radial temperature gradients on the tower scale.
2. No radiation heat transfer on the tower and PCM-sphere scales.
3. All physical properties are constant and represent overall averages.
4. The PCM is considered discretely dispersed within the continuous phase of the process fluid.

5. There is no convection in the liquid phase of the PCM.
6. The PCM is a single phase at the start of each period.

The first assumption is valid for well-insulated regenerators. The second assumption is not valid for high-temperature PCRs; however radiation in packed beds may be treated by invoking an effective radiant conductivity (see Larkin and Churchill [45]). Assumption 3 is valid in a first approximation for many systems. The fourth assumption is valid for packed beds. From the review of phase-change heat transfer, one may conclude that assumption 5 is not valid; however if the PCM is small, or if the PCM is composed of a porous matrix filled with a phase-change compound (such as described by Olszewski [42]), this assumption is valid. Assumption 6 is generally applicable if the PCR is cycled with large enough θ_x that the entire phase-change charge is spent. The final model developed need not necessarily be based upon all the above assumptions.

3.3.1. Bed Scale Description

The bed scale may be described by the axial dispersion equation (ADE). In addition to what has been presented earlier, the following nomenclature is used:

dimensionless time (·)	ϑ
process fluid dimensionless temperature (·)	t_f
fluid thermal conductivity (W/m °K)	k_f
PCM dimensionless temperature (·)	t_{PCM}
PCR axial coordinate (m)	ℓ
dimensionless axial coordinate (·)	ξ
PCR bed radius (m)	R_B
tortuosity of the packing (m fluid/m bed)	τ_B
axial Peclet number for heat transfer (·)	Pe_a
Stanton number for heat transfer (·)	St

In dimensionless form the ADE is

$$\psi \frac{\partial t_f}{\partial \vartheta} = \frac{1}{Pe_a} \frac{\partial^2 t_f}{\partial \xi^2} - \frac{\partial t_f}{\partial \xi} - St\,(t_f - t_{PCM}|_1) \tag{3.7}$$

where

$$t_f = \frac{(T_{i,h} - T_f)}{(T_{i,h} - T_{i,c})} \qquad \xi = \frac{\ell}{L}$$

$$t_{PCM} = \frac{(T_{i,h} - T_{PCM})}{(T_{i,h} - T_{i,c})} \qquad \vartheta = \psi \frac{v_f}{\epsilon_B L} \tau$$

and $t_{PCM}|_1$ represents the dimensionless temperature at the surface of the PCM sphere. The dimensionless groups are

$$Pe_a = \frac{L v_f \rho_f C_{p,f}}{k_{ef}} \qquad St = \frac{3(1-\epsilon_B) h_B L}{R_{PCM} v_f \rho_f C_{p,f}}$$

where the fluid effective thermal conductivity, k_{ef}, is given by

$$k_{ef} = \frac{k_f \epsilon_B}{\tau_B}$$

The forcing function is defined as

$$t^i = \begin{cases} 1 & \text{for heating period} \\ 0 & \text{for cooling period} \end{cases} \tag{3.8}$$

In general, the Danckwerts BCs apply:

$$\xi = 0\,; \qquad t_f - \frac{1}{Pe_a} \frac{\partial t_f}{\partial \xi} = t^i \tag{3.9.a}$$

$$\xi = 1\,; \qquad \frac{\partial t_f}{\partial \xi} = 0 \tag{3.9.b}$$

For long regenerators the Hulburt BCs may be used:

$$\xi = 0\,; \qquad t_f = t^i \tag{3.9.c}$$

$$\xi \to 1\,; \qquad \frac{\partial t_f}{\partial \xi} \to 0 \tag{3.9.d}$$

When modeling a PCR cycle, the IC is given by the final condition of the previous period, *i.e.* for the x period

$$\text{for a cocurrent PCR} \qquad t_f(0,\xi) = t_f^p(\theta_{1-x}, \xi) \tag{3.10.a}$$

$$\text{for a countercurrent PCR} \qquad t_f(0,\xi) = t_f^p(\theta_{1-x}, 1-\xi) \tag{3.10.b}$$

where $t_f^p(\vartheta,\xi)$ represents the dimensionless temperature profile at time $\vartheta = \theta_{1-x}$ for the previous period, and $1-x$ represents the subscript for the previous period (*e.g.* if $x = h$ then $1-x = c$). The IC for a single blow is obtained by replacing t_f^p with t^i.

3.3.2. PCM Scale Description

Either front-tracking or fixed-domain methods can be applied to solve the Stefan problem. Both will be described here.

3.3.2.1. Front-Tracking Method. In the front-tracking method eq. 2.9 subject to the BCs 2.10 and 2.11.a to 2.11.c is solved. Supplementing previous nomenclature, define:

dimensionless y phase temperature $(\cdot)$	t_y
dimensionless radius $(\cdot)$	φ
y-phase dimensionless inner radius in x period $(\cdot)$	$\omega_{x,y,i}$
y-phase dimensionless outer radius in x period $(\cdot)$	$\omega_{x,y,o}$
s/l-interface dimensionless radius $(\cdot)$	δ_d
Biot number $(\cdot)$	Bi

The nondimensionalized PDEs are represented by

$$\frac{1}{\varphi^2}\frac{\partial}{\partial\varphi}\left(\varphi^2\frac{\partial t_y}{\partial\varphi}\right) = \frac{3\,Bi}{St}\frac{\partial t_l}{\partial\vartheta}\ ; \qquad \omega_{x,y,i} < \varphi < \omega_{x,y,o} \tag{3.11}$$

where

$$\omega_{h,s,i} = 0 \qquad \omega_{h,s,o} = \delta_d \qquad \omega_{h,l,i} = \delta_d \qquad \omega_{h,l,o} = 1$$

$$\omega_{c,l,i} = 0 \qquad \omega_{c,l,o} = \delta_d \qquad \omega_{c,s,i} = \delta_d \qquad \omega_{c,s,o} = 1$$

with

$$\varphi = \frac{r}{R_{PCM}} \qquad\qquad \delta_d = \frac{\delta}{R_{PCM}}$$

The position of the solid/liquid interface given by δ_d is obtained by an energy-flux balance

$$\frac{\partial t_s}{\partial \varphi} - \frac{\partial t_l}{\partial \varphi} = \frac{3\,Bi}{St\,Ste}\,\frac{\rho_{PC}}{\rho_{PCM}}\,\frac{d\delta_d}{d\vartheta} \;; \qquad \varphi = \delta_d \tag{3.12}$$

The Biot number is defined as

$$Bi = \frac{h_B\,R_{PCM}}{k_{PCM}}$$

The BCs to be applied to eq. 3.11 are

$$\varphi = 0 \;; \qquad \frac{\partial t_{yi}}{\partial \varphi} = 0 \tag{3.13.a}$$

$$\varphi = \delta_d \;; \qquad t_s = t_l = t_M \tag{3.13.b}$$

$$\varphi = 1 \;; \qquad \frac{\partial t_{yo}}{\partial \varphi} = Bi(t_f - t_{yo}) \tag{3.13.c}$$

where

for a heating period	$yi = s$	$yo = l$
for a cooling period	$yi = l$	$yo = s$

Note

$$t_{PCM} = t_{yo}\Big|_{\varphi=1}$$

The IC for the PCM scale is

$$\vartheta = 0 \;; \qquad 0 \le \varphi \le 1 \;; \qquad t_{yo} = t_M \tag{3.14}$$

Equation 3.11 assumes constant and equal physical properties for the solid and liquid phases per assumption 3. Further, by assumption 4 there is only one interface during phase change. In addition, as discussed in Chapter 2, the phase-change component conductivity must be of the same order of magnitude or greater than the support-matrix conductivity for eq. 3.11 to be valid. If this is not true, a fixed-domain approach must be implemented.

3.3.2.2. Fixed-Domain Method. Alternatively, the PCM scale can be modeled using the enthalpy method. The dimensionless enthalpy function, u, is

$$u = t_{PCM} + \chi\, Ste \tag{3.15}$$

which has been derived from eq. 2.13 assuming $C_{p,PCM}$ is constant. The temperature within the PCM sphere is now given by the modified conduction equation:

$$\frac{\partial u}{\partial \vartheta} = \frac{3\,St}{Bi}\,\frac{1}{\varphi^2}\,\frac{\partial}{\partial \varphi}\left(\varphi^2\,\frac{\partial t_{PCM}}{\partial \varphi}\right) \tag{3.16}$$

The BCs are

$$\varphi = 0\,; \qquad \frac{\partial t_{PCM}}{\partial \varphi} = 0 \tag{3.17.a}$$

$$\varphi = 1\,; \qquad \frac{\partial t_{PCM}}{\partial \varphi} = Bi\,(t_f - t_{PCM}) \tag{3.17.b}$$

The IC is

$$\vartheta = 0\,; \qquad 0 \le \varphi \le 1\,; \qquad t_{PCM}(0,\varphi) = t^{p}_{PCM}(\theta_{1-x},\varphi) \tag{3.18}$$

where again the superscript p and the subscript $1-x$ denote the profile from the previous period.

Two sets of model equations for the PCR can be formulated. One set is formed from the ADE 3.7 coupled with the two PDEs represented by eq. 3.11 and the ordinary differential equation (ODE) for the solid/liquid interface, eq. 3.12. The other set is formed from the ADE coupled with one PDE 3.16 and the definition of the enthalpy function, eq. 3.15.

This concludes the presentation of preliminary work. Then next chapter outlines a research plan for achieving the objectives of this proposal.

4. Proposed Work

This final chapter is subdivided into four sections. The first section outlines an action plan for meeting the first objective: *viz.* developing models for single-blow PCRs. The second section presents a plan for achieving the second objective: modeling cyclic operation of PCRs. The third section presents an outline for reaching the third objective: experimental verification of the models. The final section presents a timetable for all proposed work.

4.1. Single-Blow Models

The model equations presented in Chapter 3 can be numerically solved by a variety of techniques. The models are based upon three independent coordinates: two spatial – the bed and the PCM, and one temporal. Discretization of one or more of the coordinates allows one to integrate along the remaining coordinate(s). Since the spatial coordinates span an *a priori* known domain, *viz.* $[0,1]$, discretization in space and integration along time, the method of lines, is a simple and often effective approach.

Regardless of how the Stefan problem is treated, the ADE must be discretized. Approaches such as collocation [46], collocation on finite elements [47] , finite elements and finite differences are applicable. For large values of Pe_a Deans and Lapidus [48] have shown that a central finite differences representation of the ADE is equivalent to the tanks-in-series representation of dispersion; thus the PDE is reduced to N (where $N = Pe_a/2$) ODEs. The PCR is modeled as N mixing cells.

The finite differences approach may be used even when Pe_a is too small to justify the tanks-in-series representation: gradients in space are converted to linear

differences of t_f at discretized ξ. In this case a compartments representation (see Wen and Fan [49]) is produced. This representation again can be assigned an analogy to well-stirred cells which are interconnected to account for forward and backward mixing.

If the fluid in the PCR is a gas the accumulation parameter, ψ, is generally very small ($\psi < 10^{-3}$). In this case the pseudo steady-state approximation may be invoked and the ADE may be further simplified to a set of N nonlinear equations.

The front-tracking formulation represented by eq. 3.11 can be discretized in space to convert the PDEs into ODEs. If the Stefan number is small (*e.g.* $Ste < 10^{-2}$) the pseudo steady-state assumption may be invoked on the PCM-sphere scale, converting the PDEs of eq. 3.11 into ODEs which can be analytically integrated. Then eq. 3.12 applied in each of the N cells would be integrated along with the tanks-in-series equations.

Another approximation which can be made is to assume that the liquid phase convection is so strong that this phase is completely mixed. In this case the temperature gradient $\partial t_l / \partial \varphi$ is zero; the temperature throughout the liquid phase must be t_M. The Stefan problem is reduced to a single-phase problem, *i.e.* the conduction problem need only be solved for the solid phase. The solid-phase spatial gradient can be handled by collocation methods. This approximation may be valid for a encapsulated PCM, but not for a supported PCM. Of course melt convection can be handled as described by Moore *et al.* [39], but the coupling of this model with the bed-scale description may be problematical.

With the front-tracking formulation one must account for sensible heat storage independently of phase-change heat storage. One technique for handling this is invoking Duhamel's Theorem [25]. For each mixing cell the temperature history while the PCM is a single phase is recorded. The convolution of the fluid temperature and a homogeneous solution to the conduction problem gives $t_{PCM}|_1$ required in the ADE or mixing-cell representation. The convolution integral may

be analytically evaluated assuming the fluid temperature is given by a cubic polynomial in time. The evaluation of $t_{PCM}|_1$ would then require fitting the history to cubic splines. Then $t_{PCM}|_1$ is obtained by substitution of the spline coefficients into the integrated expression.

The fixed-domain representation is more elegant since sensible heat storage is automatically included. A finite difference representation of the problem as described by Shamsundar and Sparrow [32] could be employed in this problem; however, instead of discretizing both temporally and spatially, one would discretize in space. On the PCM scale there would be M ODEs for each mixing cell. $N \times M$ ODEs would be integrated.

After both representations are programmed on the computer (for both gas and liquid PCR fluid) comparisons can be made between computational efforts, speed, and accuracy. Thermal efficiency can be obtained by quadrature and investigated as a function of dimensionless groups.

4.2. Modeling of Cyclic PCRs

Once computer models for single-blow operation are developed the open method of establishing cyclic equilibrium that was described in Chapter 2 may be used: the computer programs repeatedly solve the equations, cycling between hot and cold periods until the steady cycle is obtained. This procedure could be complicated with the front-tracking formulation since there may be a possibility of multiple solid/liquid interfaces if the PCR is cycled at high frequency. In addition, the temperature histories and interface positions, δ for each of the N cells, must be accounted for and rearranged when the PCR is swung.

Finding the equilibrium cycle by closed methods is more elegant. The front-tracking formulation can be used only in the approximation of no sensible heat storage. This is not practical.

A closed method approach may be attempted on the fixed-domain formulation. The discretized model consists of $M \times N$ ODEs which are linear in the $M \times N$ unknowns. Laplace transformation of the ODEs reduces the system to a set of equations. These equations are forced with a periodic function which can be represented in the Laplace domain. The equilibrium cycle is obtained by application of frequency response techniques.

Alternatively, the equations can be discretized in time as well as space. If there are O time steps there are $N \times M \times O$ equations that can be solved for the equilibrium cycle by equating one cycle to the next. The time discretization is devised so that O steps give exactly one cycle. If the step sizes are small a very large number of equations must be handled. If these equations are linear this does not pose a problem; however if they are nonlinear some linearization may be required.

Once the equilibrium cycle is found the overall efficiency can be calculated. Since it is expected the PCRs will operate with $t_M \neq 0.5$ the problem of scheduling units will need to be addressed. Analysis of the equilibrium cycle as a function of dimensionless groups will provide some insight into proper scheduling.

A key question in this analysis is how does the discretization affect the calculation of the equilibrium cycle, *i.e.* is the cycle calculated in this way the true equilibrium cycle, or does discretization introduce errors? Some effort must be made in ascertaining the answer to this question.

4.3. Experimental Verification

Experiments aimed at verifying the models developed are planned. A major task in this portion of the project is fabrication of the PCM spheres. One method would be to use a porous sphere which can retain the liquid phase by capillary forces. Such a concept was proposed by Olszewski [42] for high temperature

heat storage. Shell International Chemical Company, Ltd. manufactures a high porosity catalyst carrier which may be used. The product, Shell S-980-A, is a 3 mm dia. silica sphere with a porosity of 0.7. These spheres could be filled with 1-octadecane parafin which melts at a manageable temperature of 301.2 °K. The average pore diameter is 15 nm; the capillary pressure generated by a parafin (surface tension of 27.45 μN/m) in this pore is 7.3 kPa. The ratio of latent heat to sensible heat is $73/\Delta T$; thus in an experiment where the temperature rise is 5 °K, fifteen times more heat is stored in the phase change than in the sensible heating of the parafin and silica. The thermal conductivity of the silica matrix is approximately five times that of the wax, so the heat conduction in the PCM matrix will actually be higher than it would be in the solid wax phase. To properly model this system the effective thermal conductivity of the PCM, k_{PCM} , will have to be modified to include enhanced heat conduction. The silica-supported PCM would be stable in a gas environment; but may be unstable in many liquids because either the wax will be dissolved by the liquid, or the wax will be displaced by the liquid.

One attractive feature of this system is the visual indication of the phase: the solid is opaque, while the liquid is perfectly transparent. One may observe the movement of the melt front within the sphere, or more apropos, within the bed. Because of the small pore diameter there is no melt convection, with the exception of the small flow which may be produced because of solid/liquid density differences.

Another candidate PCM could be an inert-shell encapsulated wax. Fabrication of microencapsulated octadecane and eicosane has been reported [38]; however the diameter of these spheres (50 to 100 μm) is outside the target range of 3 mm to 7 mm dia. that is anticipated for these experiments. Some exploratory effort at fabricating encapsulated PCM should be made. If this effort is fruitful, this material could be used in model evaluation.

An alternative to conventional encapsulation would be to fill hollow spheres with a PCM. Hollow 70/30 brass (or aluminum) spheres used in making bead chain are available. The diameters of these spheres range from 2.4 mm to 9.5 mm. Because of the method of fabrication, *viz.* spinning/swaging, the wall thickness of the shell occupies 35 percent of the sphere volume. For the brass/octadecane system the ratio of latent heat to sensible heat is $54/\Delta T$. The beads have holes at the poles of the sphere. The diameter of these hole range from 1.1 mm for the smallest sphere to 2.0 mm for the largest. Once the sphere is filled, the holes can be sealed with solder or some organic adhesive/filler (*e.g.* epoxy, silicone, *etc.*). The high thermal conductivity of the metal would increase the axial conduction of heat along the length of the bed. Unless a simple method for easily sealing the holes is found, however, this alternative does not seem practical since about 5000 to 15000 of these spheres are required.

Besides these metal spheres, hollow plastic spheres are available. The smallest spheres are 10 mm in diameter and made of polypropylene or polyethylene. Estimates of wall thicknesses were not available from the manufacturer, but it is believed these spheres have a 0.5 mm thick wall. The spheres would have to be filled by a syringe. The puncture could be sealed by melting the plastic over the puncture. Unless a method for automating the filling process is found this is not practical.

Once the PCM is manufactured a PCR would be constructed. Figure 4.1 shows a sketch of the proposed apparatus. A transparent plexiglass column approximately 5 to 10 cm in diameter and 50 to 75 cm long would contain the PCM. The PCR is insulated by a vacuum jacket contained by a concentric outer tube of transparent plexiglass. O-rings pressed against flanges would seal the vacuum jacket, yet permit convenient disassembly of the unit. Flange fasteners may not be necessary since atmospheric pressure against the flange faces will compress the o-rings. Thermocouples positioned inside the column measure the temper-

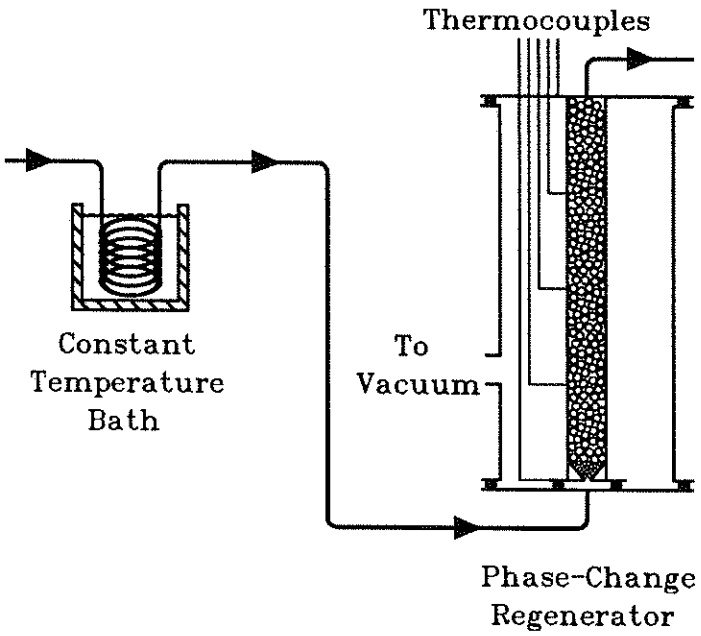

Figure 4.1 Sketch of experimental apparatus.

ature profile. A data acquisition computer will be used to read and store this information.

The fluid is introduced at the bottom of the column and distributed by a low heat capacity distributor: either hollow glass beads, or the S-980-A beads. Fluid is maintained at a constant temperature by flowing it through coils immersed in a constant temperature bath. In the case of cycling regenerators, two constant temperature baths are used and a valve selects the temperature of the PCR inlet fluid. For experiments in countercurrent cycling an additional distributor must be positioned at the top of the PCR.

Data acquired during the experiment consists of temperature profiles and fluid outlet temperature. In addition, phase change may be observed if the PCM undergoes a transition from opaque to transparent; the front position as a function of time can be recorded in this case.

At this point the optimal PCM can be selected. The working model describing

this material will be established. Comparison between the model and experimental data can then be made. Both temperature profiles and thermal efficiencies can be calculated. The experimental PCR equilibrium cycle can be compared against the calculated cycle.

4.4. Timing

It is planned this research will be completed by the end of the year. Table 4.1 presents estimates for the time required to complete the work.

Table 4.1
Timetable for research

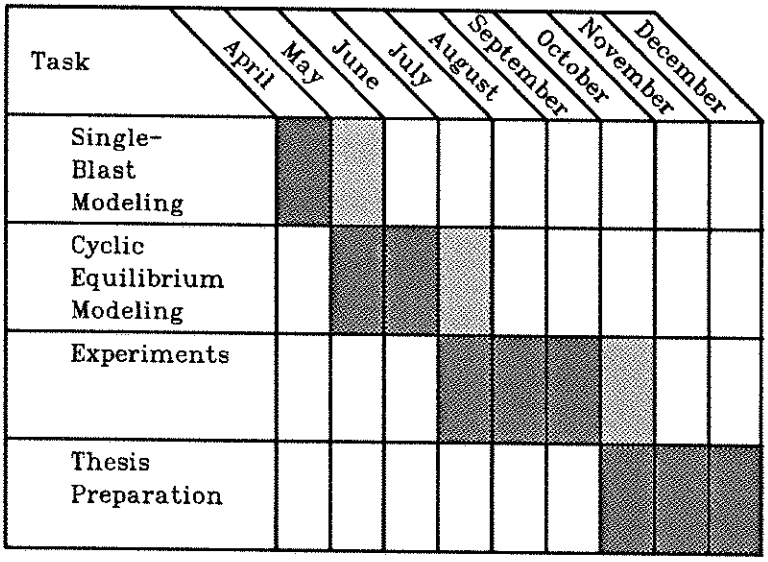

This concludes the presentation of proposed work.

5. Nomenclature

Acronyms

ADE	Axial Dispersion Equation
PC	Phase-change Component
PCM	Phase-Change Materials
PCR	Phase-Change Regenerator
SC	Support-matrix Component

Symbols

Bi	Biot number; p. 36
C_p	heat capacity, J/kg °K
h	convective heat transfer coefficient, W/m^2 °K
k	thermal conductivity, W/m °K
L	regenerator length, m
ℓ	regenerator axial length coordinate, m
$\dot{m}$	fluid mass flowrate, kg/s
N	number of mixing cells
Pe	Peclet number for heat transfer; p. 34
Q	heat energy, J
R	maximum radius, m
r	spherical coordinate, m
St	Stanton number for heat transfer; p. 34
Ste	Stefan number; p. 26
T	temperature, °K
t	dimensionless temperature; eq. 2.5
U	enthalpy function, J/kg; eq. 2.13
u	enthalpy function; eq. 3.15
v	fluid superficial velocity, m/s

Greek Symbols

δ	melt front coordinate, m
ϵ	porosity, m^3/m^3
φ	sphere coordinate; p. 35
η	efficiency; eq. 2.3
κ	period fraction; eq. 3.6
λ	latent heat of fusion, J/kg
μ	temperature break-though time; p. 26
χ	melt fraction; p. 21

ρ	density, m^3/kg
τ	time coordinate, s
$\mathcal{T}$	tortuosity, m/m
θ	regenerator period, s
ϑ	time coordinate; p. 34
ψ	accumulation parameter; p. 26
ω	domain endpoint; p. 35
ξ	regenerator axial coordinate; p. 34

Subscripts[†]

a	axial
B	bed
c	cooling period
d	dimensionless
f	fluid
h	heating period
i	inlet [first][‡]; inner [third]
l	liquid phase
M	melting point
o	outlet [first]; outer [third]
PC	phase-change component
PCM	PCM (effective) property
PCR	PCR (regenerator) property
p	packing (for C_p apply to [second] only)
SC	support-matrix component
s	solid phase
x	generic for h and c
y	generic for s and l
yi	generic for inner phase s or l
yo	generic for outer phase s or l
z	generic for SC or PC
$1-x$	opposite of x

Superscripts

i	initial
id	ideal
o	overall
p	previous

[†]Multiple subscripts are separated by commas.

[‡]Brackets designate the position of the subscript.

6. Bibliography

[1] Gunn, Marvin E., "Recovery of Industrial Waste Heat", in *Utilization of Reject Heat*, ch 2, Mitchell Olszewski, editor, Marcel Dekker, Inc., New York, 1980.

[2] Hunt, V. Daniel, *Handbook of Conservation of Solar Energy, Trends and Perspectives*, ch 2, Van Nostrand Reinhold Company, New York, 1982.

[3] Lane, George A., *Solar Heat Storage: Latent Heat Materials. Volume I: Background and Scientific Principles*, ch 1, CRC Press, Boca Raton, Florida.

[4] Reiter, Sydney, *Industrial and Commercial Heat Recovery Systems*, ch 4, Van Nostrand Reinhold Company, Inc., Cincinnati, 1983.

[5] Reay, D. A., *Heat Recovery Systems – A directory of equipment and techniques*, Halsted Press, New York, 1979.

[6] Hausen, Helmuth, *Heat Transfer in Counterflow, Parallel Flow and Cross Flow*, chs 11-19, translated from German by M. S. Sayer, edited by A. J. Willmott, McGraw-Hill, Inc., New York, 1983.

[7] Davies, Mansel, *The Physical Principles of Gas Liquefaction and Low Temperature Rectification*, pp. 93-109 and pp. 125-134, Longmans, Green and Co., London, England 1949.

[8] Schmidt, F. W. and A. J. Willmott, *Thermal Energy Storage and Regeneration*, Hemisphere Publishing Corporation, New York, 1981.

[9] Levenspiel, Octave, *Chemical Reaction Engineering*, Second edition, ch 9, John Wiley & Sons, Inc., New York, 1972.

[10] Jakob, Max, *Heat Transfer, Volume II*, ch 35, John Wiley & Sons, Inc., New York, 1957.

[11] Nusselt, W., "Die Theorie des Winderhitzers," *Z. Ver. deut. Ing.* **71**, 85 (1927).

[12] Anzelius, A., "Über Erwärmung vermittels durchströmender Medien," *Z. Angew. Math. Mech.* **6**, 291 (1926).

[13] Schumann, T. E. W., "Heat Transfer: A Liquid Flowing Through a Porous Prism," *J. Franklin Inst.* **208**, 405 (1929).

[14] Klinkenberg, A., "Heat Transfer in Cross-Flow: Heat Exchangers and Packed Beds," *Ind. Eng. Chem.* **46**, 2285 (1954).

[15] Larsen, Floyd W., "Rapid Calculation of Temperature in a Regenerative Heat Exchanger Having Arbitrary Initial Solid and Entering Fluid Temperatures," *Int. J. Heat Mass Transfer* **10**, 149 (1967).

[16] Handley, D. and P. J. Heggs, "The Effect of Thermal Conductivity of the Packing Material on Transient Heat Transfer in a Fixed Bed," *Int. J. Heat Mass Transfer* **12**, 549 (1969).

[17] Schmidt, F. W. and J. Szego, "Transient Response of a Hollow Cylindrical-Cross-Section Solid Sensible Heat: Storage Unit – Single Fluid," and "Analysis of the Effects of Finite Conductivity in the Single Blow Heat Storage Unit," *J. Heat Transfer* **100**, 737 and 740 (1978).

[18] Burch, D. M., R. W. Allen and B. A. Peavy, "Transient Temperature Distributions Within Porous Slabs Subjected to Sudden Transpiration Heating," *J. Heat Transfer* **98**, 221 (1976).

[19] Lai, Shin-Ming, *Periodic Operation of Heat Regenerators: A New Method for Calculation of Thermal Efficiency*, Master of Science Dissertation, Washington University, St. Louis, Missouri, 1983.

[20] Lu, P. -C., "Single-Blow Transients in Packed-Bed Storage Units With Solid-Phase Conduction by Crump's Numerical Inversion of Laplace Transforms," *J. Heat Transfer* **105**, 493 (1983).

[21] Ackermann, G., "Die Theorie der Wärmeaustauscher mit Wärmespeicherung," *Z. Angew Math. Mech.* **11**, 192 (1931).

[22] Nahavandi, A. N. and A. S. Weinstein, "A Solution to the Periodic-Flow Regenerative Heat Exchanger Problem," *Appl. sci. Res.* **10**, 335 (1961).

[23] Kardas, Alan, "On a Problem in the Theory of the Unidirectional Regenerator," *Int. J. Heat Mass Transfer* **9**, 567 (1966).

[24] Willmott, A. J., "The Regenerative Heat Exchanger Computer Representation," *Int. J. Heat Mass Transfer* **12**, 997 (1969).

[25] Carslaw, H. S. and J. C. Jaeger, *Conduction of Heat in Solids*, Second Edition, pp 30-33, pp 240-241, ch XI, Oxford University Press, Great Britain, 1959.

[26] Crank, John, *Free and moving boundary problem*, chs 3-6, Clarendon Press, Oxford, 1984.

[27] Muehlbauer, John C. and J. Edward Sunderland, "Heat Conduction with Freezing or Melting," *Appl. Mech. Rev.* **18**, 951 (1965).

[28] Mori, A. and K. Araki, "Methods for analysis of the moving boundary-surface problem," *Int. Chem. Eng.* **16**, 734 (1976).

[29] Furzeland, R. M., "A Comparative Study of Numerical Methods for Moving Boundary Problems," *J. Inst. Maths. Applics.* **26**, 419 (1980).

[30] Schneider, G. E. and M. J. Raw, "An Implicit Solution Procedure for Finite Difference Modeling of the Stefan Problem," *AIAA J.* **22**, 1685 (1984).

[31] Chawla, T. C., D. R. Paddersen, G. Leaf, W.J. Minkowycz and A. R. Shoumann, "Adaptive Collocation Methods for Simultaneous Heat and Mass Diffusion With Phase Change," *J. Heat Transfer* **106**, 491 (1984).

[32] Shamsundar, N. and E. M. Sparrow, "Analysis of Multidimensional Conduction Phase Change Via the Enthalpy Model," *J. Heat Transfer* **97**, 333 (1975).

[33] Cambell, S., in *Energy Utilization: A Sourcebook of Current Technology*, ch 56, The Fairmont Press, Inc., Atlanta Georgia, 1980.

[34] Katayama, K., Akio Saito, Yoshio Utaka, Akihiro Saito, Hideo Matsui, Hiromichi Maekawa, and A. Z. A. Saifullah, "Heat Transfer Characteristics of the Latent Heat Thermal Energy Storage Capsule," *Solar Energy* **27**, 91 (1981).

[35] Rieger, H., U. Projahn, M. Bareiss, H. Beer, "Heat Transfer During Melting Inside a Horizontal Tube," *J. Heat Transfer* **105**, 226 (1983).

[36] El-Masry, Said El-Sayed, "Numerical Investigation of Phase Change Heat Transfer in a Horizontal Cylinder Including Effects on Natural Convection," Ph. D. dissertation, University of Miami, Coral Gables, Florida, May, 1984.

[37] Mulligan, J. C., "Phase-Change Heat-Storage Module," *NASA Tech Briefs* **13**, 103 (1989).

[38] NASA Technical Support Package MFS-26071, "Phase-Change Heat-Storage Module," available through NASA Scientific and Technical Information Facility, Washington D. C. (1989).

[39] Moore, F. E. and Y. Bayazitoglu, "Melting Within a Spherical Enclosure," *J. Heat Transfer* **104**, 19 (1982).

[40] Morrison, D. J. and S. I. Abdel-Khalik, "Effects of Phase-Change Energy Storage on the Performance of Air-Based and Liquid-Based Solar Heating Systems," *Solar Energy* **20**, 57 (1978).

[41] Bliem, C., D. J. Landini, J. F. Whitbeck, R. Kochan, J. C. Mittl, R. Piscitella, J. Schafer, A. Synder, D. J. Wiggins, J. M. Zabriskie, B. A. Barna, S. P. Henslee, P. V. Kelsey, J. I. Federer and E. S. Bomar, *Ceramic Heat Exchanger Concepts and Materials Technology*, pp. 33-38, pp. 153-154 and pp. 171-199, Noyes Publications, Park Ridge, New Jersey, 1985.

[42] Olszewski, M., "Advanced Latent Heat Storage Media for High-Temperature Industrial Applications," NTIS, document no. DE 85000907, 1984.

[43] Arimilli, Rao V., "Modeling of Transient Heat Transfer in Packed Beds," in *Proceedings of the U. S. D. O. E. Thermal Energy Storage Program Review: Report to Industry*, March 11-12, 1987.

[44] Adebiyi, Geaoge A., "Development of PCM Packed Bed Thermal Model for Industrial Applications," in *Proceedings of the Diurnal/Industrial Thermal Energy Storage Research Activities Review*, March 9-10, 1988.

[45] Larkin, Bert K. and Stuart W. Churchill, "Heat Transfer by Radiation through Porous Insulations, " *A.I.Ch.E. J.* **5**, 467 (1959).

[46] Villadsen, John and Michael L. Michelsen, *Solution of Differential Equation Models by Polynomial Approximation*, chs 3-4 and 8-9, Prentice-Hall, Inc., Englewood Cliffs, New Jersey, 1978.

[47] Madsen, N. K. and R. F. Sincovec, "ALGORITHM 540 PDECOL, General Collocation Software for Partial Differential Equations [D3], " *ACM Trans. Math. Soft.* **5**, 326 (1979).

[48] Deans, H. A. and Leon Lapidus, "A Computational Model For Predicting and Correlating the Behavior of Fixed-Bed Reactors: I. Derivation of Models for Nonreacting Systems," *A.I.Ch.E. J.* **6**, 656 (1960).

[49] Wen, C. Y. and L. T. Fan, *Models for Flow Systems and Chemical Reactors*, ch 7, Marcel Dekker, New York, 1975.

WASHINGTON UNIVERSITY
SEVER INSTITUTE OF TECHNOLOGY

HEAT REGENERATORS WITH PHASE-CHANGE MATERIALS

By

Henry F. Erk

Prepared under the direction of Professor M. P. Duduković

A proposal presented to the Sever Institute of
Washington University in partial fulfillment
of the requirements for the degree of

DOCTOR OF SCIENCE

April, 1990

Saint Louis, Missouri

WASHINGTON UNIVERSITY
SEVER INSTITUTE OF TECHNOLOGY

ABSTRACT

HEAT REGENERATORS WITH PHASE-CHANGE MATERIALS

by Henry F. Erk

ADVISOR: Professor M. P. Duduković

April, 1990

Saint Louis, Missouri

A research project exploring heat recovery and storage in tower regenerators packed with phase-change material is discussed. Such phase-change regenerators (PCRs) could be used in many applications, ranging from storage of solar energy for domestic heating to providing a source of high-temperature blast gas in the metalurgical industries.

A review of conventional heat regenerators, including an equipment survey and survey of mathematical models, is presented. The Stefan problem, *i.e.* the mathematical treatment of phase-change heat conduction and storage, is discussed; solution methods are reviewed. A literature survey of mathematical and experimental research on phase-change heat storage is presented.

The concept of an ideal PCR is introduced and modeled. Thermal efficiency for the ideal case is presented. The mathematical modeling of PCRs is discussed. Equations describing the energy and temperature profiles within a PCR are presented. Equations describing the cyclically operated PCR are presented.

A research plan containing a balanced combination of mathematical modeling and experimentation is presented. Methods for numerically solving the model equations are discussed. An approach for calculating the equilibrium-cycle temperature response for a periodically cycled PCR is outlined. Experiments focused on ascertaining the validity of the models are described.

TABLE OF CONTENTS

LIST OF FIGURES

LIST OF TABLES

1. Introduction

1.1. Motivation

Recently thermal energy users have been compelled to reduce fuel consumption. Two factors are responsible:

- economic — the depletion of nonrenewable, low-cost energy sources results in the conversion to more expensive fuels;
- legislative — the imposition of emission standards for pollutants such as SO_x, NO_x, and CO_x forces reduction in fuels burned.

These two constraints hit energy consumers in the pocketbook: higher fuel costs and higher capital costs for pollution control equipment. The only means of reducing fuel consumption while maintaining capacity is to improve energy utilization efficiency.

As if this were not enough, another constraint is being imposed which encourages energy conservation, *i.e.*

- legislative — the imposition of maximum temperature levels for effluent and exhaust forces additional heat recovery from waste streams.

Gunn [1][†] estimates that approximately eleven percent of the energy consumed in the manufacturing sector is rejected as waste heat. Clearly there is a need to improve waste-heat recovery technology.

There is also great pressure in the private sector to reduce fuel consumption. The energy crises of the seventies, *i.e.* the Arab oil embargo of 1973 and the turmoil in Iran which began in 1978, have underscored the importance of developing alternative energy sources. A large amount of fossil fuel is consumed for

[†]The numbers in braces refer to references in the bibliography.

residential/commercial heating: either directly in the form of burning coal, oil, or natural gas; or indirectly through the use of electricity which is generated from fossil fuel. Hunt [2] estimates that in the United States thirty-seven percent of the total energy demand is for residential/commercial use. Of this percentage fifty-two percent is used for space heating and nine percent is used for water heating. Thus domestic heating accounts for nearly twenty percent of the energy consumed in the United States.

The use of solar energy has long been proposed as an alternative energy source for domestic heating. Unfortunately the cyclic supply of radiant solar energy does not always match the thermal energy demand. Techniques for providing a buffer between the supply and demand are required. One of the most efficient of these techniques is latent heat storage: the thermal energy generated from solar radiation is stored in the reversible phase change of a substance. The concept of latent heat storage for domestic heating applications is almost sixty years old [3], yet this is not utilized extensively today.

Faced with the stark reality of ever-diminishing fossil fuel supplies, and the recognition of all the costs associated with using fossil fuels, it is apparent that there is a need to improve thermal energy storage and recovery technology. Substitution of latent heat for sensible heat in conventional heat storage/recovery equipment is one improvement which could reduce consumption of fossil fuel with virtually no equipment modification.

Consider the fixed-bed heat regenerator, a mainstay of thermal energy storage (TES), where energy is stored in the sensible heat of the packing material. Greater amounts of energy could be stored at near isothermal conditions if the packing were replaced by an encapsulated phase-change material (PCM). The concept of PCM heat storage has been explored for low surface-area-to-volume geometry, *e.g.* pipes filled with PCM. However the rate of heat storage is limited by solid/liquid interfacial area. The heat storage rate per unit volume is low. In this case

increasing the surface area to volume ratio by discretely distributing PCM, *e.g.* filling the regenerator with spheres of PCM, makes sense. This concept has not been extensively explored in the open literature and there is a clear need for modeling and experimental studies to ascertain its effectiveness.

This proposal outlines a course of research conducted to answer salient questions related to the phase-change heat regenerator (PCR). PCRs have applications in industry, for heat conservation and recovery; and in effectively utilizing solar energy for domestic heating applications.

1.2. Objectives

The objectives of this research project center around developing an understanding of how PCRs perform. Specifically, the following items are proposed:

1. Develop a mathematical model for a fixed-bed heat regenerator which utilizes an encapsulated or supported PCM. Investigate the single-blow thermal efficiency as a function of operating parameters and compare results with those predicted for conventional sensible-heat regenerators.
2. Investigate cyclic operation of a PCR. Devise methods for calculating the steady-state or equilibrium cycle. Explore the overall thermal efficiency of this regenerator and compare with a conventional regenerator.
3. Experimentally validate models on a small-scale laboratory regenerator. If discrepancies exist between model and experiment ascertain why and suggest refinements.

The remainder of this proposal is divided into three chapters. The next chapter presents background material and cursory literature reviews. Chapter 3 presents a discussion of preliminary work. The final chapter presents a discussion of the proposed work.

2. Background

This chapter is divided into two sections. The first section reviews conventional heat regenerators describing the advantages and disadvantages of these devices; key parameters and models for regenerators are then presented. The second section begins by presenting a brief review of techniques for solving the Stefan problem, *i.e.* the problem of heat transfer with phase change. The section concludes with a review of the literature on phase-change heat storage.

2.1. Heat Regenerators

Before reviewing pertinent regenerator theory we shall examine the advantages and disadvantages of regenerators relative to other conventional heat recovery equipment.

2.1.1. Equipment Survey

Basically there are two types of heat recovery devices: recuperators and regenerators. Recuperators are heat exchangers; heat is transferred from the waste stream through the wall and then finally into the process stream. Regenerators are heat storage devices as well as heat exchangers; heat is transferred from the waste stream into storage media, and later transferred from the storage media to a process stream. The simplest regenerator is a tower which is packed with high heat-capacity packing. For high temperature applications the packing may be refractory brick arranged in the form of a checkerwork.

Table 2.1 gives a comparison between recuperators and tower regenerators. Regenerators offer high heat transfer areas per unit volume, high heat transfer

Table 2.1

Comparison Between Regenerators and Recuperators[‡]

Attribute	Regenerator Tower	Recuperator
stores heat	yes	no
heat supply	cyclic	continuous
outlet stream temperature	varying	constant
heat transfer	direct	indirect
ease of turndown	easy	difficult
heat transfer area/volume	high	low
thermal efficiency	medium	high
ease of fabrication	easy	difficult
relative capital cost	low	medium
handling solid laden streams	easy	difficult
subject to fouling	no	yes

[‡]Comparison based upon information in Reiter [4] and Reay [5]

rates, a wide operating range, and can effectively operate at very high or very low temperatures. A major deficiency of regenerators is the inability to deliver a uniform and continuous supply of heat efficiently.

Regenerators are used in high temperature applications with abrasive (*e.g.* soot laden) streams. For example regenerators are utilized to recover waste heat from flue gas, using the energy to preheat incoming burner air in fired boilers. In these applications the walls of a recuperator would have to be made from exotic alloys or ceramics, formed in complex geometries. With continuous long-term operation the abrasive soot may erode holes into the recuperators walls, degrading performance. On the other hand a tower regenerator is fabricated from the same materials, but built from simple shapes; *e.g.* bricks, spheres, rings, saddles, *etc.* which can be relatively inexpensive to manufacture. Abrasive soot will erode the packing within tower regenerators, but this does not influence the performance.

Regenerators are utilized as a high temperature heat supply for the metalur-

gical and glass-manufacture industries where heat is required in cycles for batch processing. For example, Cowper stoves 50 m tall and 11 m in diameter have been used to supply 500,000 m^3/h of high temperature (1000 to 1300°C) blast gas for iron smelting [6]. The cyclic nature of regenerators compliments the heat requirements for these batch processes. Unfortunately, regenerators do not supply a constant temperature which may be desirable, *e.g.* for heat soaking bricks; some energy is wasted because the regenerator is operated at an average temperature in excess of the required temperature.

Regenerators have been used in place of heat exchangers in gas separation and liquefaction. For this application the packing consists of thin, highly conductive, metal strips which are wound radially within the tower. Here the regenerator acts as a feed air purifier as well [7]. Process vent gas and feed gas alternately flow through the tower. When the cold, expanding vent gas flows through the tower, packing temperature drops to a low temperature as the gas is heated. After several minutes valves redirect the streams so that now the feed gas flows countercurrently through the tower. Water, carbon dioxide, and other condensible gases freeze on the packing while the feed gas is cooled. The feed air is thus purified. Condensibles are flushed out by the vent gas during the next cycle.

Two or more regenerators may be coupled together for continuous energy recovery. In the simplest configuration two units are interconnected via manifolds and valves so that one regenerator is absorbing energy from the hot process stream while the other regenerator is releasing energy to the cold process stream. The time during which the unit stores energy from the hot process fluid is called the heating period, while the time during which the unit releases energy to the cold process stream is called the cooling period. The units are piped so that each regenerator may be cycled, or swung, between heating and cooling periods. For this configuration to be efficient, the length of the heating period should be equal to that of the cooling period. In this case, the two regenerators are alternately

cycled so that one of the two units is in a heating period while the other is in a cooling period.

Two modes of regenerator operation exist in this configuration:

- countercurrent or counterflow, and
- cocurrent or parallel.

Figure 2.1 shows schematics of these two modes. In countercurrent operation the

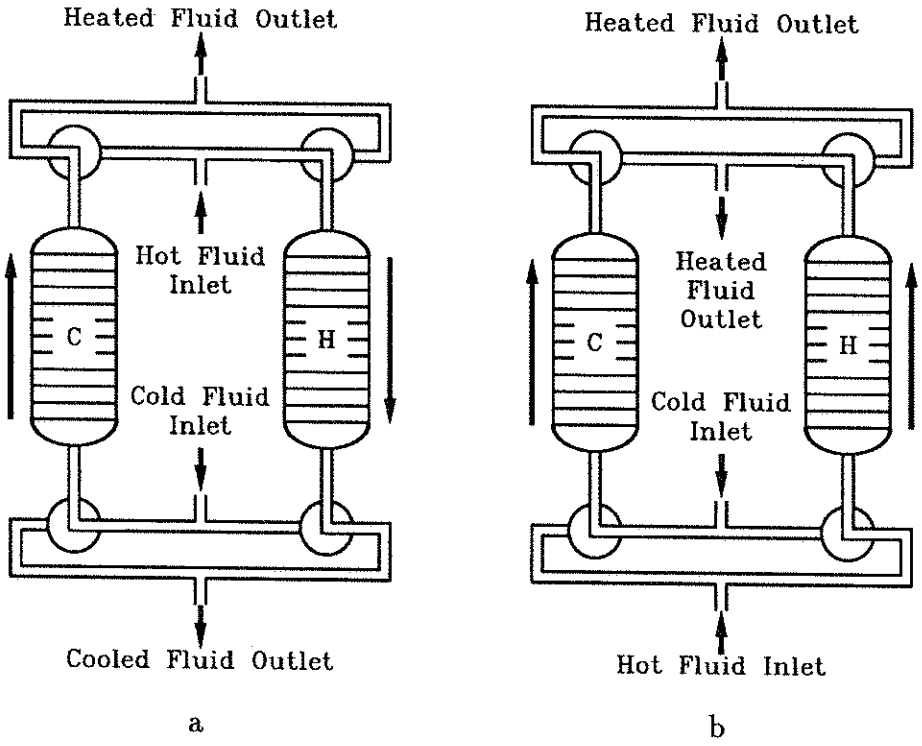

Figure 2.1 Continuous packed-tower regenerators. Fig 2.1.a: countercurrent or counterflow. Fig 2.1.b: cocurrent or parallel flow. The regenerators labeled 'C' are in a cooling period. The regenerators labeled 'H' are in a heating period.

process streams flow in reverse directions through the unit, *i.e.* during the heating period the hot-process stream flows in one direction and during the cooling period the cold-process stream flows in the other direction (*e.g.* in Fig. 2.1.a the hot-process stream flows downward while the cold-process stream flows upward). Four

three-way valves cycle the units through alternating heating and cooling periods. For example in Fig. 2.1.a when the regenerators are to be swung the four valves rotate ninety degrees counterclockwise; the right-hand regenerator swings from heating period into cooling period and the left-hand unit swings from cooling period into heating period.

Flow reversal can be an advantage when one of the process streams is dirty or contains significant amounts of a component which may condense and/or freeze on the packing or checkerwork. In this case channels in the regenerator may become clogged, however, when the flow is reversed the debris is backflushed out of the unit [8].

Analogous to counterflow heat exchangers, counterflow regenerators transfer heat with a more or less uniform gradient throughout the length of the bed. In a heating period hot fluid enters the bed at the warmest end (the top of the bed in Fig. 2.1.a) and exits at the coolest. In a cooling period cold fluid enters at the coolest end and exits at the warmest.

Figure 2.1.b shows the cocurrent mode of regenerator operation. In this mode the hot and cold process streams flow in the same direction through the unit, *e.g.* upward in Fig. 2.1.b. By rotating the four three-way valves ninety degrees counterclockwise the right-hand regenerator swings from heating period to cooling period, while the left-hand regenerator swings from cooling period to heating period. In contrast to countercurrent regenerators, cocurrent regenerators may suffer from plugging when processing dirty streams. Analogous to parallel flow heat exchangers, the temperature gradient in a counterflow regenerator is the greatest at the inlet and the smallest at the outlet.

A variation of the packed tower regenerator is the rotary regenerator: the Ljungstrom [4] or Munter wheel [5] and the Rothemuhle regenerator [4]. Figure 2.2.a shows a schematic of the Ljungstrom wheel. A checkered-matrix wheel rotates at 1–20 rpm. within a split duct. The hot stream flows through one side of

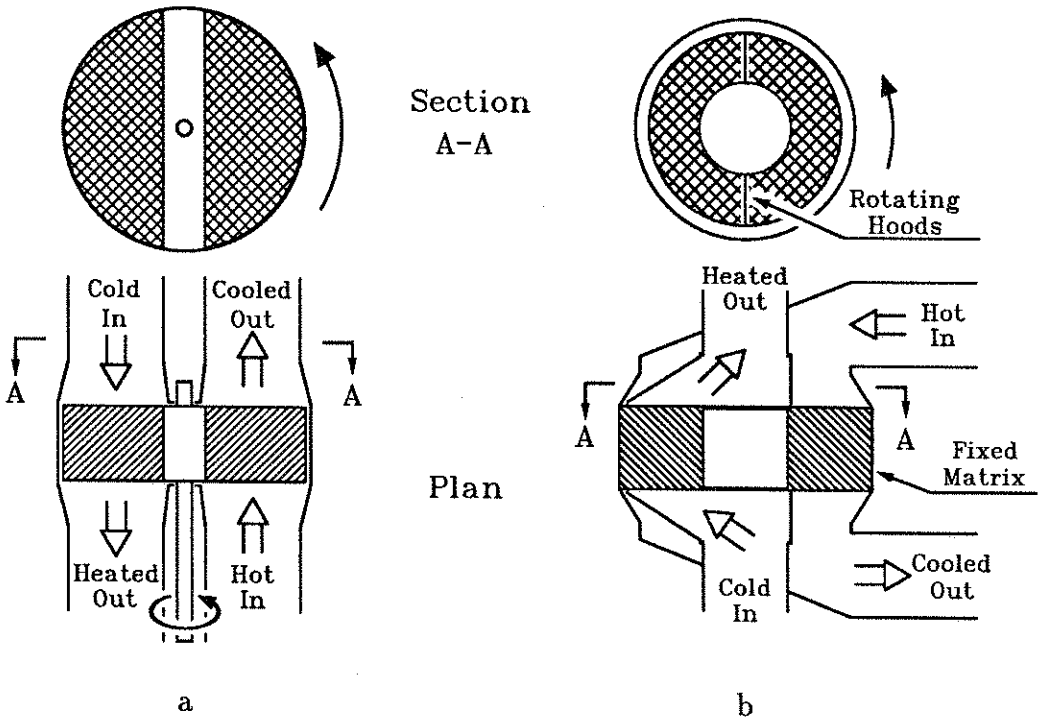

Figure 2.2 Rotary regenerators. Fig. 2.2.a: Ljungstrom regenerator. Fig. 2.2.b: Rothemuhle regenerator. Adapted from [5].

the duct, while the cold flows though the other side. The portion of the matrix in contact with the hot process stream is heated; the absorbed heat is released when this section of the wheel rotates into the cold stream duct. Flexible circumferential seals and face seals minimize cross-stream contamination in low temperature applications. In high temperature applications no seals are used at all. To minimize contamination the pressure difference between the two streams must be limited to approximately 10 kPa. With this limitation contamination is kept to below 0.5 percent for low temperature units and 4 percent for high temperature units. In applications where contamination cannot be tolerated a purge flow may be used. This flow is directed through a duct which lies between the two process ducts. Heat transfer is regulated by varying the rotation speed of the wheel as well as stream flows.

In the Rothemuhle regenerator, Fig. 2.2.b, instead of a rotating wheel inside stationary ducts, there is a stationary matrix with rotating hoods which act as moving ducts. Flexible seals may be used in low temperature applications to minimize contamination.

The rotary regenerator is used in power plants and steam generation facilities to recover heat from burner exhaust gas. In Europe they are also used to pre-condition air temperature and humidity in building heating, ventilation and air conditioning (HVAC) applications. Rotary regenerators offers high heat transfer capacity at relatively low costs. A major drawback with these devices is some cross-stream contamination. [5].

Further information on regenerators can be found in Reay [5], who presents a compendium of regenerator equipment, manufacturers and specifications.

Summarizing our review of heat recovery devices: regenerators have advantages over recuperators in applications where heat demand and/or supply is cyclic or intermittent. Regenerators can be effective in very high or very low temperature applications, especially when process streams are dirty. Despite the fact that regenerators must be cycled, multiple regenerators can be operated to provide continuous heat supply. Continuous regenerators such as the Ljungstrom wheel or the Rothemuhle regenerator are useful in heat recovery applications.

2.1.2. Regenerator Models

Parameters for regenerator operation will now be presented. A review of models for heat regenerators follows.

2.1.2.1. Parameters. Major regenerator parameters are the fluid exit temperature and the thermal efficiency. The regenerator temperature profile may also be of interest. If the regenerator is used for heat recovery, efficiency is the key

parameter. If however the regenerator is used as a heat supply, outlet temperature is the key parameter. In general one of the parameters is optimized at the expense of the other, *e.g.* a regenerator optimized to maximize efficiency may not be effective as a constant-temperature heat supply. Regenerator models are formed from energy balances, so the temperature profile and outlet temperature may be obtained. Thermal efficiency (or effectiveness) is calculated from the outlet temperature history. Efficiency is defined as the ratio of the amount of energy which has been exchanged to the total amount of energy which theoretically could be exchanged.

Consider a single packed-tower heat regenerator at a constant, uniform temperature which is subject to a step-change in inlet fluid temperature. We wish to describe the single-blow (or single-blast) efficiency. Define the following notation:

process fluid inlet temperature (°K)	$T_{i,x}$
process fluid outlet temperature (°K)	$T_{o,x}$
process fluid heat capacity (J/kg °K)	$C_{p,x}$
process fluid mass flowrate (kg/s)	$\dot{m}_x$
period duration (s)	θ_x
energy stored during period (J)	Q_x
period efficiency (·)	η_x
the running time coordinate (s)	τ

where the subscript x is replaced by h for a hot blast and by c for the cold blast. Figure 2.3 shows how the outlet fluid temperature varies between $T_{i,h}$ and $T_{i,c}$ over several heating and cooling periods for this typical regenerator.

In calculating single-blow thermal efficiencies one assumes that at the end of the period the regenerator packing is in thermal equilibrium with process fluid.

During any blast the total amount of heat which is absorbed by the packing, Q_x, is the total change in the sensible heat of the process fluid; *viz.*:

$$Q_x = \pm \dot{m}_x C_{p,x} \int_0^{\theta_x} (T_{i,x} - T_{o,x}) \, d\tau \tag{2.1}$$

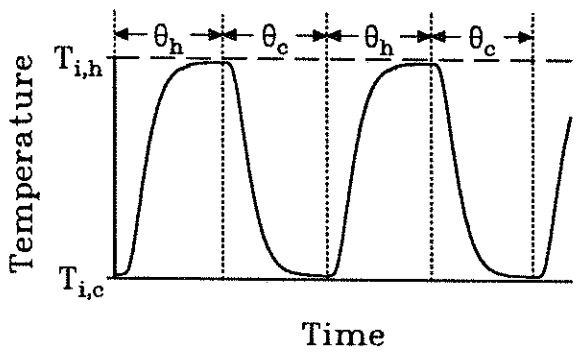

Figure 2.3 Typical regenerator outlet-fluid temperature history.

where for a hot blast $x \rightarrow h$ and the + sign in front of the integral applies; for a cold blast $x \rightarrow c$ and the − sign applies. The ideal, thermodynamics-limited, amount of heat which the regenerator can store, Q_x^{id}, is given by the energy difference between the hot-process fluid and the cold-process fluid, *viz.*:

$$Q_x^{id} = \dot{m}_x \, C_{p,x} \, \theta_x \, (T_{i,h} - T_{i,c}) \tag{2.2}$$

The preceding two equations are based upon the assumptions that $\dot{m}_x$ and $C_{p,x}$ are constant or are overall integral-averaged values.

The single-blow thermal efficiency is

$$\eta_x \equiv \frac{Q_x}{Q_x^{id}} \tag{2.3}$$

On substituting eq. 2.1 and eq. 2.2 into eq. 2.3 and simplifying, one obtains

$$\eta_x = \frac{\pm \int_0^{\theta_x} (T_{i,x} - T_{o,x}) \, d\tau}{\theta_x \, (T_{i,h} - T_{i,c})} \tag{2.4}$$

Equation 2.4 may be further simplified if one changes the temperature scale. Define a dimensionless temperature scale by

$$t = \frac{(T_{i,h} - T)}{(T_{i,h} - T_{i,c})} \tag{2.5}$$

e.g. $t_{o,h}$ is the dimensionless temperature for $T = T_{o,h}$. This scaling maps the actual temperature range onto the interval $[0,1]$. Now for a hot blast eq. 2.4 becomes

$$\eta_h = \frac{\int_0^{\theta_h}(1 - t_{o,h})\,d\tau}{\theta_h} \tag{2.6}$$

The hot-period single-blow thermal efficiency is given by dividing the area above the thermal **F** curve by the length of the period. This curve is the dimensionless response to a step-up change in inlet conditions. Levenspiel [9] has defined the **F** curve in terms of concentration, here temperature is substituted. Figure 2.4 shows a typical **F** curve for a hot blast. When a regenerator operates at high

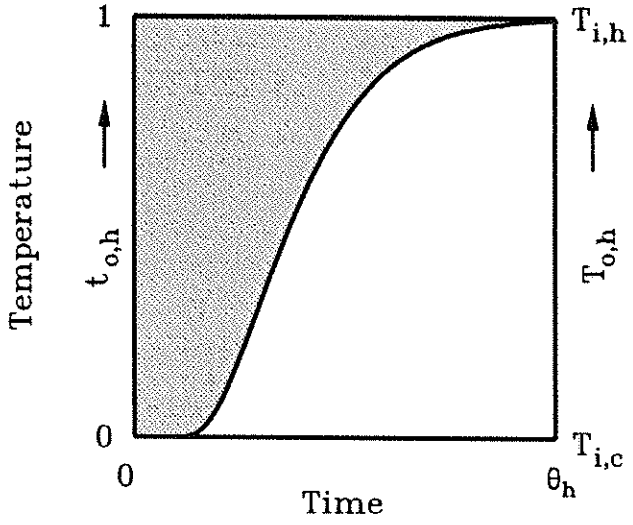

The shaded area is given by the integral:

$$\int_0^{\theta_h}(1 - t_{o,h})\,d\tau\ .$$

Larger shaded areas indicate higher efficiencies. Here the efficiency is approximately 0.44.

Figure 2.4 Typical **F** curve for a regenerator in a heating period.

efficiency the area above the curve will be large, *i.e.* $t_{o,h}$ will be close to zero, indicating a large fraction of the energy available in the process fluid has been stored in the unit.

For a cold blast eq. 2.4, simplified in terms of the dimensionless temperature, is

$$\eta_c = \frac{\int_0^{\theta_c} t_{o,c}\,d\tau}{\theta_c} \tag{2.7}$$

In this case the efficiency is given by the area under the **W** curve divided by the length of the period. The **W** curve is the dimensionless response to a step-down change in inlet conditions. For this linear system **W = 1-F**.

Figure 2.5 shows a typical **W** curve for a regenerator in a cooling period. In

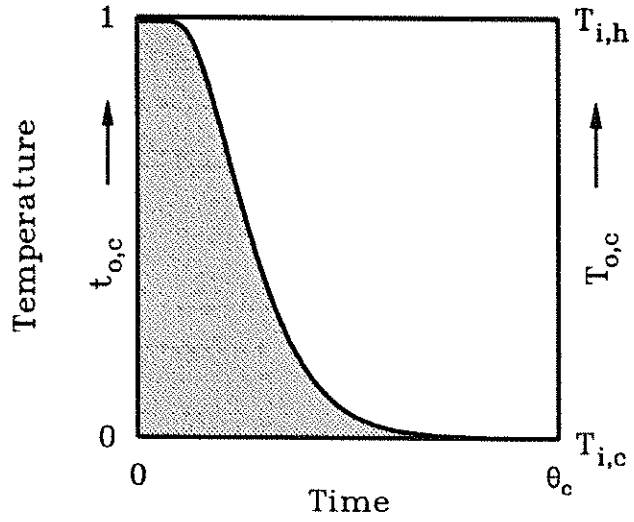

The shaded area is given by the integral:

$$\int_0^{\theta_h} t_{o,c}\, d\tau \ .$$

Larger shaded areas indicate higher efficiencies. Here the efficiency is approximately 0.29.

Figure 2.5 Typical **W** curve for a regenerator in a cooling period.

the cooling period, when a regenerator is operating at high efficiency, the area below the curve will be large, *i.e.* $t_{o,c}$ will be close to one. This indicates that a large fraction of the energy has been transferred to the cold process fluid.

In practice the regenerator period is not long enough to assure thermal equilibrium between the process fluid and the packing. Regenerators are swung at or before thermal breakthrough. In this case the packing temperature is not uniform; efficiency is not given by the single-blow value. The overall efficiency of the regenerator, η^o is defined:

$$\eta^o \equiv \frac{Q_h + Q_c}{Q_h^{id} + Q_c^{id}} \tag{2.8}$$

The definition of η^o parallels that of the single-blow efficiencies, although strictly speaking the responses are no longer **F** and **W** curves.

2.1.2.2. Models. The classical mathematical treatment of regenerators has been summarized by Jakob [10], Hausen [6], and Schmidt and Willmott [8]. Models for single blow operation can be written for six ideal cases:

1. The regenerator periods are essentially zero and the regenerator is cycled infinitely fast.
2. The packing thermal conductivity is infinite.
3. The packing thermal conductivity is infinite along the regenerator axis and finite along the cross section.
4. The packing thermal conductivity is zero along the axis and infinite along the cross section.
5. The packing thermal conductivity is zero along the axis and finite along the cross section.
6. The packing thermal conductivity is finite along the axis and zero along the cross section.

Cases 1 and 2 are not realistic. Case 3 is applicable only for short regenerators with heavily insulated walls; one of limited use. Case 4 describes low-temperature regenerators used in gas liquefaction. Cases 5 and 6 describe high-temperature regenerators used in metalurgical and glass industries. Either case 5 or 6 can describe a regenerator which contains a checkerwork or random packing.

Nusselt [11] discussed the first five cases. He considered only convective-film heat transfer and neglected temperature gradients within the packing. This simplifying assumption was also used by Anzelius [12], Hausen (described in [6]), and Schumann [13] who each independently presented solutions of case 4. The simplified model of case 4 is often referred to as the Schumann model. Klinkenberg [14] has reviewed both numerical and analytic solutions for the Schumann model. Larsen [15] presents a numerical approximation.

Nusselt [11] described an approximate solution method using a finite difference scheme for the case 5. Handley and Heggs [16] present a numerical solution for a packed bed, under the conditions of case 5 including the effects of intraparticle

conduction and film convection. Schmidt and Szego [17] describe a finite-elements solution for regenerator channels also including these effects.

Case 6 has been solved numerically by Burch *et al.* [18] using finite differences and Lu [20] who numerically inverted the Laplace-transform analytical solution. Both Burch *et al.* and Lu assumed that heat transport due to fluid flow is negligible. Lai [19] presents and approximate solution for case 6 as a function of the mean and variance of the impulse response.

All the preceding models have considered single-blow operation. To predict the overall efficiency and performance of a swing regenerator it is necessary to calculate the equilibrium cycle. Here a cycle is defined as a hot blow followed by a cold blow.

The analysis of the periodic cycling of regenerators follows two different approaches: the closed method and the open method. To apply the closed method a closed-form solution, either exact or approximate, is obtained for the model equations; *e.g.* cases 1 through 6, for one cycle. This solution is a function of the initial condition (IC), *i.e.* the temperature profile within the regenerator; thus the solution for a given cycle depends upon the solution of the previous cycle. Cyclic equilibrium requires that the solution for one cycle is equal to the solution for the next. Equating two successive cycles allows one to find this.

To apply the open method a model is evaluated for a cycle. At the end of the cycle the current conditions are used as the IC for the next cycle and the model is solved again. This process iterates until repeatable cycles evolve. The model is cycled just as the regenerator. Assuming the model is not chaotic, the equilibrium cycle is reached.

Nusselt [11] described a closed method analysis for a countercurrent regenerator modeled as case 4. Ackermann [21] extended the analysis and found the solution in terms of a Fourier series and another series which was obtained by

application of Volterra integral equations. Nahavandi and Weinstein [22] also present a closed-method solution, using an infinite series representation of the solution's IC and solving for the constants of this series.

Hausen [6] reviews equilibrium cycle calculations. He describes a complex closed method analysis using eigenfunctions for cocurrent and countercurrent regenerators described by case 4. Kardas [23] has performed a closed-method analysis for cocurrent regenerators described by case 5. Lai [19] performed closed-method analyses for packed bed regenerators (case 6) for both cocurrent and countercurrent operation.

The work of Willmott [24] is a typical application of the open method. Willmott simulated a regenerator described by case 4 using a finite difference scheme. He started the computation with an IC which he hoped approximated that of the equilibrium cycle and began the simulation. After several simulated cycles the calculations converged.

All the models considered here are linear and techniques such as superposition can be applied to establish the equilibrium cycle. Unfortunately, when one considers phase-change heat storage the model is no longer linear.

This completes the review of heat regenerators. The next section presents a review of phase-change heat transfer.

2.2. Phase-Change Heat Storage

The mathematical description for transient heat transfer with a phase change is called the Stefan problem in honor of J. Stefan who studied this problem in the 1890's. A review of methods for solution of this problem is now presented. A review of phase-change heat transfer follows.

2.2.1. Stefan Problem Solution Techniques

Consider a PCR filled with spherical PCM. Assume the PCM is composed of two components: a matrix of inert material (support component) filled with a heat storage substance (phase-change component). Both components have finite heat capacity and thermal conductivity. The equations which follow are valid for a heating period where the PCM changes from solid to liquid. A similar analysis can be performed for the cooling period but is not presented here. Define the following terms:

y-phase temperature (°K)	T_y
PC melting temperature (°K)	T_M
fluid temperature around PCM sphere (°K)	T_f
z-component density (kg/m^3)	ρ_z
z-component heat capacity (J/kg °K)	$C_{p,z}$
z-component thermal conductivity (W/m °K)	k_z
convective transfer coefficient (W/m^2 °K)	h_B
PC latent heat of fusion (J/kg)	λ
spatial coordinate — radius (m)	r
PCM sphere radius (m)	R_{PCM}
PCM support porosity (m^3 PC/m^3 PCM)	ϵ_{SC}
SC tortuosity (m pore/m radius)	τ_{SC}

where the subscript y is replaced by l to designate liquid phase and s to designate solid phase, and the subscript z is replaced by SC to designate support component and PC to designate phase-change component. Assuming the physical properties of the phase-change component are constant and equal for both phases, the effective PCM properties are

$$\rho_{PCM} = \rho_{PC}\,\epsilon_{SC} + \rho_{SC}\,(1-\epsilon_{SC})$$

$$C_{p,PCM} = \frac{C_{p,PC}\,\rho_{PC}\,\epsilon_{SC} + C_{p,SC}\,\rho_{SC}\,(1-\epsilon_{SC})}{\rho_{PCM}}$$

$$k_{PCM} = \frac{1}{\tau_{SC}}\left[k_{PC}\,\epsilon_{SC} + k_{SC}\,(1-\epsilon_{SC})\right]$$

The expression for k_{PCM} assumes that the matrix tortuosity is equal to the pore tortuosity. This assumption is valid for an open-pore structure with uniform-thickness walls and narrow pore-size distribution.

The energy balance for each phase is the classical Fourier equation:

$$C_{p,PCM}\,\rho_{PCM}\,\frac{\partial T_y}{\partial \tau} = k_{PCM}\,\frac{1}{r^2}\,\frac{\partial}{\partial r}\left(r^2\frac{\partial T_y}{\partial r}\right) \quad \begin{cases} 0 < r < \delta & y = s \\ \delta < r < R_{PCM} & y = l \end{cases} \tag{2.9}$$

Equation 2.9 is based upon the assumptions that physical properties are constant and equal for both phases, and that there is no liquid-phase convection. To incorporate convection one must augment the energy equation with a momentum-balance equation, *e.g.* the Navier-Stokes equation.

The position of the solid/liquid interface, δ, is given by a heat flux balance:

$$k_{PCM}\,\frac{\partial T_s}{\partial r} - k_{PCM}\,\frac{\partial T_l}{\partial r} = \lambda\,\rho_{PC}\,\epsilon_{SC}\,\frac{d\,\delta}{d\,\tau}\,; \qquad r = \delta \tag{2.10}$$

If solid and liquid densities are not equal, a convective term must be added to eqs. 2.9 and 2.10. Equation 2.10 is valid when the support conductivity is of the same order of magnitude as (or less than) the conductivity of the phase-change component. If the support conductivity is much greater than the conductivity of the phase-change compound, heat is conducted by the matrix throughout the entire sphere faster than it is consumed by phase change. A flat temperature profile develops within the sphere. The solid/liquid interface is parallel to the pore walls of the matrix. The mathematical description of this interface is very complex and cannot be described by eq. 2.10

When eqs. 2.9 and 2.10 are applicable the boundary conditions (BCs) are:

$$r = 0\,; \qquad k_{PCM}\frac{\partial T_s}{\partial r} = 0 \tag{2.11.a}$$

$$r = \delta\,; \qquad T_s = T_l = T_M \tag{2.11.b}$$

$$r = R_{PCM}\,; \qquad k_{PCM}\frac{\partial T_l}{\partial r} = h_B\,(T_f - T_l) \tag{2.11.c}$$

The IC is:

$$\tau = 0\,; \qquad 0 \leq r \leq R_{PCM}\,; \qquad T_s(r) = T^i(r) \tag{2.12}$$

where $T^i(r)$ represents the initial temperature profile in the PCM.

Because this problem consists of two coupled partial differential equations (PDEs) with a moving boundary, an analytical solution on the finite domain exists only for simple cases [25]. The analytical solution of Neumann [25] applies for the semi-infinite slab. Crank [26] describes other solutions.

Reviews by Muehlbauer and Sunderland [27], and Mori and Araki [28] do not present analytical solutions for spherical geometry with the BCs given above. To the best knowledge of this author, an analytical solution for this problem has not been reported.

Approximate methods for solving the Stefan problem may be grouped into two categories: front-tracking and fixed-domain. In front-tracking methods eq. 2.10 is solved along with the (PDEs) represented by eq. 2.9. Numerical methods such as finite differences, finite elements, orthogonal collocation, collocation on finite elements, *etc.* are employed to discretize either the spatial or temporal coordinate; or both. For example, Furzeland [29] discusses methods which discretize in time or space using finite differences. Schneider and Raw [30] describe the application of finite differences in space. Chawla *et al.* [31] present a spatial collocation method in which the collocation points move with the melt interface. In some instances the solid/liquid interface is immobilized (dividing r by δ), however this cannot be considered a fixed-domain method because δ must still be computed via the flux balance, eq. 2.10.

In fixed-domain methods the energy balance is treated differently. The latent heat is introduced into the energy balance as an enthalpy term or as a modified heat capacity. The most frequently used technique for implementing this method is to invoke an enthalpy function, U which is

$$U(T) = \int_{T_{i,c}}^{T} C_{p,PCM}(T)\, dT \; + \; \chi\, \lambda\, \epsilon_{SC} \tag{2.13}$$

where

$$\begin{aligned} &\text{for} \quad T_y < T_M \qquad \chi = 0 \\ &\text{for} \quad T_y = T_M \qquad 0 \le \chi \le 1 \\ &\text{for} \quad T_y > T_M \qquad \chi = 1 \end{aligned}$$

The contribution to the energy balance due to latent heat of fusion is taken up in a change in enthalpy. Since the phase change occurs at T_M the enthalpy function automatically brings latent heat into the conduction equation, which becomes

$$\rho_{PCM} \frac{\partial U}{\partial \tau} = k_{PCM} \frac{1}{r^2} \frac{\partial}{\partial r} \left(r^2 \frac{\partial T_{PCM}}{\partial r} \right) \; ; \qquad 0 < r < R_{PCM} \tag{2.14}$$

where T_y is replaced by T_{PCM} to emphasize that there is only a single PDE to be solved. Note that eq. 2.13 *cannot* be substituted into eq. 2.14 since differentiation of χ would give a Dirac delta function at the τ where $T_{PCM} = T_M$. Equation 2.14 must be solved together with eq. 2.13. The BCs are given by eqs. 2.11.a and 2.11.c with the subscripts s and l on T replaced by *PCM*. The IC is given by eq. 2.12 (with s replaced by *PCM*) or

$$\tau = 0 \; ; \qquad 0 \le r \le R_{PCM} \; ; \qquad U(r) = U^i(r) \tag{2.15}$$

where $U^i(r)$ represents the initial enthalpy profile.

Shamsundar and Sparrow [32] have discussed implementation of this method. Furzeland [29] and Schneider and Raw [30] have presented numerical examples of the enthalpy method implementation as well. Furzeland [29] reports that front-tracking methods are more accurate than the enthalpy method. In instances where the phase-change front geometry is complex, *e.g.* a highly conductive support matrix, front-tracking methods may be impossible to implement.

In summary: an analytical solution for the Stefan problem under the conditions applicable in a PCR has not been reported. An approximate solution or a numerical solution must be used. In terms of a numerical solution both the front-tracking and fixed-domain methods can be useful. Front-tracking methods may be slightly more accurate. Front-tracking methods cannot be used when the support-matrix conductivity is much greater than that of the phase-change component. Fixed-domain methods are simpler to implement and account for both sensible and latent heat storage in one equation.

2.2.2. Phase-Change Heat Storage Survey

Heat storage using PCM contained in tubes has been extensively explored. In fact a 6 foot long, $3\frac{1}{2}$ inch diameter polyethylene tube filled with Thermal 81® (a stabilized $CaCl_2$ manufactured by Dow Chemical — m.p. of 29.7 °C) which is sealed on both ends is a commercially available product for solar energy storage applications [33].

Katayama *et al.* [34] reported experiments using high aspect ratio tubes filled with naphthalene ($C_{10}H_8$). Experimental results were compared with a front-tracking model which is solved numerically *via.* using an implicit finite difference scheme. The model underpredicted heat storage rate. It was concluded that convection strongly influences heat transfer.

Rieger *et al.* [35] have presented a numerical and experimental investigation of phase-change heat storage in low aspect ratio tubes. Their model includes convective effects, but assumes the solid phase remains fixed in the center of the tube. Model predictions were matched to experiments, using n-octadecane ($C_{18}H_{38}$) as the phase-change material. The model did not properly describe heat transfer in the bottom section of the tube: the solid phase sank to the bottom of the tube (due to density differences between phases) and this effect was not included in the model.

El-Masry [36] presents a model based upon the front-tracking method which includes convection and melt buoyancy effects. He compares model predictions with the data presented by Katayama *et al.* [34] and Rieger *et al.* [35]. Model predictions match the experiments well. El-Masry's model reveals that melt convection can increase heat transfer rates by as much as a factor of two.

Mulligan [37] has described a phase-change heat-storage module for load-leveling of heating utilities in orbiting spacecraft. Heat is stored in a slurry of microencapsulated wax spheres. Eicosane and octadecane spheres with a diameter of 50–100 μm were fabricated with a polymer outer shell for the slurry [38]. There are no public-domain references available on modeling this system.

Phase-change heat transfer within a spherical enclosure have been investigated by Moore and Bayazitoglu [39]. Transparent glass spheres (approximately 3.3 and 2.8 cm diameter) were filled with n-octadecane wax. Visual observations of the melt front could be made. A front-tracking model was written which included convection and solid/liquid phase buoyancy effects. These effects were significant, increasing the heat transfer rates by as much as thirty percent.

Models for a channel-type phase-change heat regenerator were presented by Morrison and Abdel-Khalik [40]. They used the enthalpy method to account for phase-change heat storage. Four models were presented:

1. Case 5 with PCM.
2. Zero thermal conductivity for the PCM and fluid in all directions and zero fluid heat capacity.
3. Model 2 with no convective heat transfer resistance to the channel walls.
4. Model 3 except fluid heat capacity is not zero.

Models 1 and 4 apply when the fluid is a liquid; models 2 and 3 apply when the fluid is a gas. Using the parameters specified in [40] model 4 is a good approximation of model 1 and model 3 is a good approximation of model 2.

A method of storing high-grade heat (approximately 1000 °C) was proposed in [41]. This concept is illustrated in Figure 2.6. The phase-change material is cycled between two towers as a liquid or solid shot. In a shot tower heat is

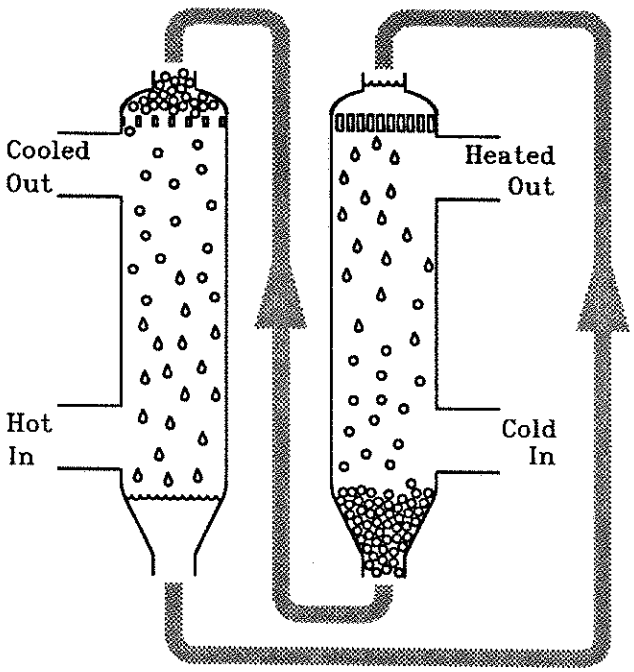

Figure 2.6 High-temperature phase-change heat storage concept.

released to the cold process gas; the molten shot solidifies. The shot are then transferred to another tower where they are contacted with the hot process gas; the shot melts, absorbing heat. The liquid is then recycled to the shot tower. The advantage of this process is that heat transfer is continuous. Major disadvantages include moving solids, pumping high-temperature liquids. This also requires a large process volume.

Olszewski [42] proposed methods for producing encapsulated and supported PCM which could be used in a high-temperature PCR. One concept was a self-encapsulating PCM which is produced by solidifying a silicon-aluminum alloy in a shot tower. During controlled solidification a silicon-rich shell forms around

the aluminum-rich molten core. Since there are opposing Si and Al concentration gradients, the melting point of the alloy decreases moving to the center. Within a temperature range the central core can be melted while the outer shell remains solid. Another concept proposed in [42] is the use of high porosity bricks which are filled with high melting-temperature PCM; the liquid phase is retained by capillary forces.

Arimilli [43] presented calculations for a spherical PCM which is composed of a porous matrix filled with a phase-change alloy. He reports the results for only one case: heat recovery from combustion gases. Unfortunately he does not describe how the calculations were performed, nor does he present details of how phase change was modeled. Adebiyi [44] presents a model for cylindrical PCM in a PCR. His model consists of an equation describing energy transport by fluid convection in the bed. Phase change in the PCM-cylinders, which are treated as spheres of an equivalent diameter, is modeled using the enthalpy method. A few results are presented for a specific application: heat storage in the manufacture of bricks. No other references to PCR models or experiments have been found.

A review of the literature has indicated that no one has systematically and thoroughly quantified all the processes which occur in a PCR. There has been no experimental verification of PCR models. Thus, there is a need to develop a methodology for predicting PCR performance in single-blow and cyclic operation and to experimentally verify the methods developed.

3. Preliminary Work

In accordance with the first objective of this research project a model for a phase-change regenerator needs to be formulated. Before developing the equations an idealized model will be explored.

3.1. Ideal PCR

Consider the ideal regenerator. The characteristic times for all heat transfer and storage processes are much smaller that the characteristic time for temperature convection by bulk flow. Figure 3.1 shows the outlet temperature history for both the ideal sensible-heat regenerator and the ideal PCR. In this figure $\mu_{s,x}$ and $\mu_{l,x}$ ($x = c$ or h) are the thermal break-through times . The subscript s designates sensible heat storage and l designates latent heat storage. These times are a measure of the heat storage capacity.

Define the nomenclature:

PCR tower length (m)	L
process fluid superficial velocity (m/s)	v_f
y phase density (kg/m^3)	ρ_y
y phase heat capacity (J/kg °K)	$C_{p,y}$
porosity of regenerator bed (m^3/m^3)	ϵ_B
accumulation parameter (·)	ψ
Stefan number (·)	Ste

where the subscript y is replaced by f for fluid properties, p or PCM for the regenerator packing (p for sensible-heat storage packing and PCM for phase-change material packing). The two dimensionless groups, Ste and ψ are defined as

$$\psi = \frac{\epsilon_B \rho_f C_{p,f}}{(1-\epsilon_B)\rho_p C_{p,p}} \qquad Ste = \frac{C_{p,PCM}(T_{i,h} - T_{i,c})}{\lambda \epsilon_{SC}}$$

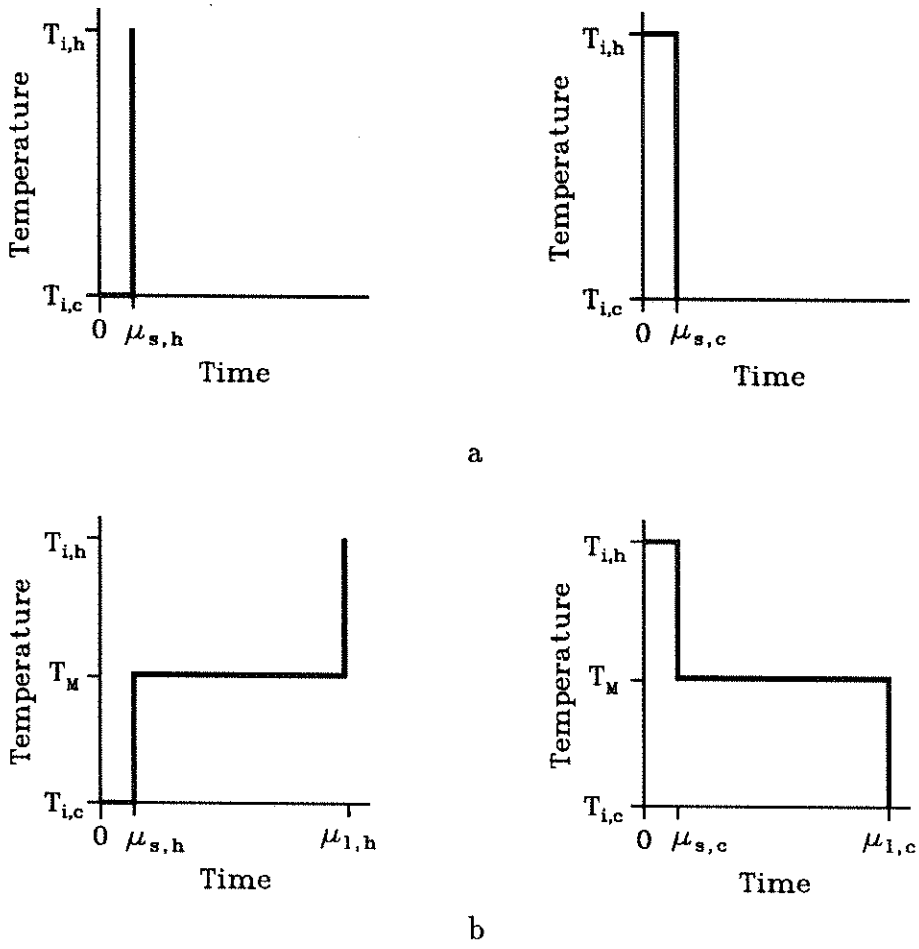

Figure 3.1 Ideal regenerator temperature histories. Fig 3.1.a : ideal sensible-heat regenerator. Fig 3.1.b : ideal PCR. Note $\mu_{s,h}$ and $\mu_{s,c}$ are the same for both figures. In each figure the left plot represents a heating period and right plot represents a cooling period.

The Stefan number, Ste, is the ratio of sensible heat to latent heat. When $Ste \rightarrow \infty$ sensible heat storage dominates, while when $Ste \rightarrow 0$ latent heat storage dominates. The accumulation parameter, ψ, is the ratio of the sensible heat of the fluid to that of the packing. When the fluid is a gas $\psi \rightarrow 0$, when the fluid is a liquid ψ is $\mathcal{O}(1)$.

The break-through times are given by:

$$\mu_{s,x} = (1+\psi)\frac{L\,\rho_p\,C_{p,p}}{v_f\,\rho_f\,C_{p,f}} \tag{3.1}$$

and

$$\mu_{l,h} = \mu_{s,x}\left[1+\frac{1}{Ste\,(1-t_M)(1+\psi)}\right] \tag{3.2.a}$$

$$\mu_{l,c} = \mu_{s,x}\left[1+\frac{1}{Ste\;t_M\;(1+\psi)}\right] \tag{3.2.b}$$

where t_M is the dimensionless temperature defined by eq. 2.5. Equations 3.2.a and 3.2.b indicate the capacity of a PCR is enhanced relative to that of a conventional unit. For a given capacity the volume occupied by a PCR is much smaller than that occupied by a conventional regenerator. A smaller unit is less expensive to build. For example, the volume required to store solar thermal energy in domestic heating applications using sensible heat may be prohibitively large. Using latent heat storage (with $Ste << 1$) the volume can be reduced to a manageable size. In high temperature applications (such a metalurgical, glass, brick, and chemical processing) a conventional regenerator which has been converted to a PCR, simply by replacing the packing with PCM, could be operated for much longer periods before being swung. The service life of the high-temperature switching valves could be increased substantially, reducing maintenance and downtime.

From Fig. 3.1 and using eqs. 2.6 and 2.7 one may derive the ideal single-blow efficiencies:

$$\eta_h = \frac{(1-t_M)\,[Ste\,(1+\psi)\;+\;1]}{Ste\,(1+\psi)\,(1\;-t_M)\;+\;1} \tag{3.3.a}$$

$$\eta_c = \frac{t_M\;[Ste\,(1+\psi)+1]}{Ste\;\;t_M\,(1+\psi)\;+\;1} \tag{3.3.b}$$

When $Ste \rightarrow \infty$, *i. e.* pure sensible heat storage, the efficiencies approach unity. When $Ste \rightarrow 0$, *i. e.* pure latent heat storage, the efficiencies are

$$\eta_h = 1 - t_M \tag{3.4.a}$$

$$\eta_c = t_M \tag{3.4.b}$$

PCR single-blow efficiencies are less than those for the ideal sensible-heat storage regenerator. Based upon this comparison one may argue that PCRs are not an effective means of reducing energy consumption. However three points must be noted. First, the actual efficiency of conventional regenerators is never one; the efficiency can be as low as 0.65 [5]. Real regenerators are never ideal, nor or they operated in single-blow mode. Second, since PCRs can store more heat per unit volume they may be used in applications where today heat is not recovered. For example, solar energy storage is not implemented because of the prohibitively large volumes required for sensible heat storage. PCRs however may make heat storage viable, saving energy which would not be utilized. Third, PCRs can provide an isothermal heat supply which is required in certain processes. Regenerators may be used instead of recuperators for the reasons discussed in Chapter 2, *e.g.* high-temperature, dirty process streams. Here PCRs can supply heat at a constant temperature which *is* the target process temperature. With conventional regenerators the lowest supply temperature must be near the target temperature, so the unit must be operated at an average temperature *higher* than the target temperature, requiring extra energy. This is illustrated in Figure 3.1. Here regenerators are used to supply process heat rather than to recover heat. Below a certain temperature the energy is useless with respect to the process. In this situation other heat recovery devices and heat integration must be used in conjunction with PCRs to improve the thermal efficiency of the overall plant rather than the specific process.

Consider the ideal PCR as a constant-temperature gas supply. Further, we

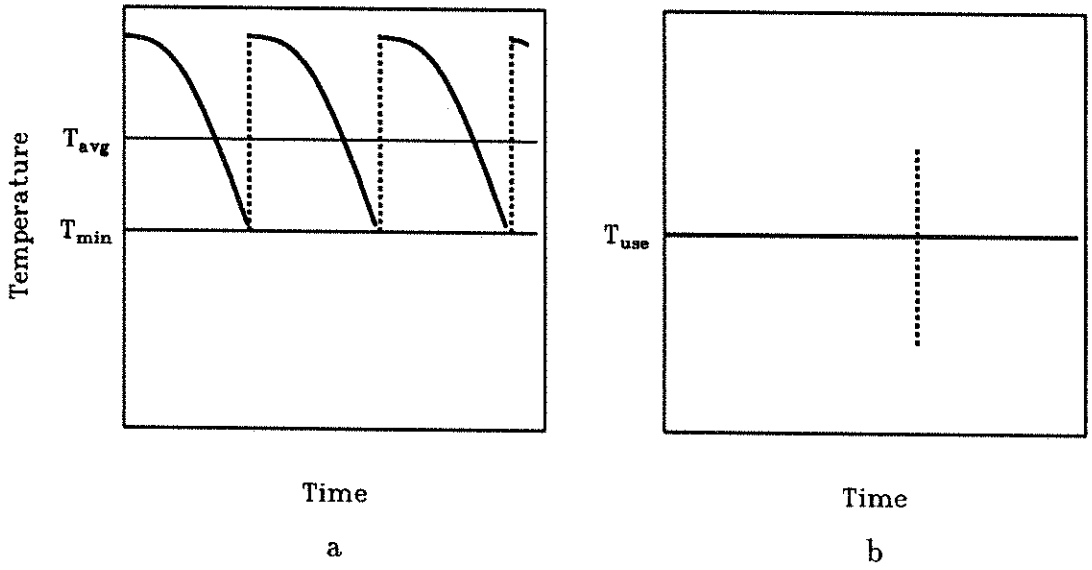

Figure 3.2 Energy savings using PCR regenerators. Fig 3.1.a : temperature history of a sensible-heat regenerator used as a constant-temperature heat supply. Fig 3.1.b : temperature history of a PCR used as a constant-temperature heat supply. $T_{use} = T_{min} = T_M$ for this process. The dashed lines in both figures indicates a swing to another regenerator.

assume Ste is zero, *i.e.* pure latent heat storage. Physical properties are assumed to be constant, and both process streams are flowing at the same rate. The amount of energy retained by the regenerator during a heating period must be equal to the amount of energy released by the regenerator during a cooling period, *viz.*

$$\theta_h \eta_h = \theta_c \eta_c \tag{3.5}$$

Normally one would want to have $\theta_h = \theta_c$. In this case the regenerator is balanced and two regenerators can be cycled as illustrated in Figure 2.1. Thus the regenerator must operate with a t_M of 0.5. Unfortunately this is not always possible nor desirable. When $t_M \neq 0.5$ the regenerator is unbalanced. A *modus operandi* for managing continuous processing must be established.

Borrowing a technique used with conventional regenerators, one may still ef-

fectively operate unbalanced regenerators. The two periods are selected so that one is an integer multiple, κ, of the other; *vis-à-vis* $\theta_h = \kappa\theta_c$ or $\theta_c = \kappa\theta_h$. In this case $\kappa + 1$ regenerators can be connected together to provide continuous processing. Assuming equal v_f for both streams, κ is

$$\left.\begin{aligned} \kappa &= \frac{(1 - t_M)}{t_M} \qquad t_M < 0.5 \\ \kappa &= \frac{t_M}{(1 - t_M)} \qquad t_M > 0.5 \end{aligned}\right\} \tag{3.6}$$

For example, for $t_M = 0.25$ $(\kappa = 3)$ one may use 4 regenerators: one in a heating period, θ_h, and three in a cooling period, $\theta_c = 3\theta_h$. Each of the three regenerators is offset in time from the others by an integer multiple of θ_h, *i.e.* at time τ the first of the three has been operating for τ, the second for $\tau + \theta_h$, the third for $\tau + 2\theta_h$. When the regenerator in the heating period is swung one of the other regenerators is ready to take its place.

This analysis indicates that efficient operation of PCRs will require multiple units which must be properly scheduled. Importance is placed on developing a methodology which can predict θ_x.

3.2. Real PCR

Four heat transfer processes exist in the PCR:

1. Heat convection by fluid flow
2. Dispersion of heat by fluid conduction.
3. Heat convection through the film (thermal boundary layer) surrounding the PCM.
4. Heat conduction/convection in the PCM.

In an ideal PCR the first process is so slow that it alone regulates overall heat transfer. Processes 2–4 reach equilibrium since their heat transfer rates are much greater than the overall rate which is set by process 1. Thus the thermodynamic-limited amount of heat, Q_x^{id}, can be transferred and $\eta_x = 1$.

For a real PCR the first process may not necessarily control the overall rate. For example, a high thermal conductivity fluid will carry energy from the inlet to the outlet of the PCR without allowing it to be stored in the PCR. Poor heat transmission to the PCM, or within the PCM, will reduce the rate of heat storage so that more heat is carried out.

The temperature history may be altered dramatically if one or more of the resistances in processes 2 to 4 dominates. To calculate the correct history the effect of all these processes must be incorporated in a detailed mathematical model. Upon an examination of the solutions from this model one may be able to develop a simpler treatment for PCRs. A major step in this direction is developing a model.

3.3. PCR Model Equations

Consider a PCR which is composed of a tower packed with uniform, spherical PCM. To model this one must account for events which occur on two scales: the tower or bed scale, and the PCM-sphere scale. Two interfaces must be accounted for: the process-fluid/PCM (intraparticle) and the solid-PCM/liquid-PCM (inter-particle). The following assumptions will be made:

1. No radial temperature gradients on the tower scale.
2. No radiation heat transfer on the tower and PCM-sphere scales.
3. All physical properties are constant and represent overall averages.
4. The PCM is considered discretely dispersed within the continuous phase of the process fluid.

5. There is no convection in the liquid phase of the PCM.
6. The PCM is a single phase at the start of each period.

The first assumption is valid for well-insulated regenerators. The second assumption is not valid for high-temperature PCRs; however radiation in packed beds may be treated by invoking an effective radiant conductivity (see Larkin and Churchill [45]). Assumption 3 is valid in a first approximation for many systems. The fourth assumption is valid for packed beds. From the review of phase-change heat transfer, one may conclude that assumption 5 is not valid; however if the PCM is small, or if the PCM is composed of a porous matrix filled with a phase-change compound (such as described by Olszewski [42]), this assumption is valid. Assumption 6 is generally applicable if the PCR is cycled with large enough θ_x that the entire phase-change charge is spent. The final model developed need not necessarily be based upon all the above assumptions.

3.3.1. Bed Scale Description

The bed scale may be described by the axial dispersion equation (ADE). In addition to what has been presented earlier, the following nomenclature is used:

dimensionless time (·)	ϑ
process fluid dimensionless temperature (·)	t_f
fluid thermal conductivity (W/m °K)	k_f
PCM dimensionless temperature (·)	t_{PCM}
PCR axial coordinate (m)	ℓ
dimensionless axial coordinate (·)	ξ
PCR bed radius (m)	R_B
tortuosity of the packing (m fluid/m bed)	τ_B
axial Peclet number for heat transfer (·)	Pe_a
Stanton number for heat transfer (·)	St

In dimensionless form the ADE is

$$\psi \frac{\partial t_f}{\partial \vartheta} = \frac{1}{Pe_a} \frac{\partial^2 t_f}{\partial \xi^2} - \frac{\partial t_f}{\partial \xi} - St\,(t_f - t_{PCM}|_1) \tag{3.7}$$

where

$$t_f = \frac{(T_{i,h} - T_f)}{(T_{i,h} - T_{i,c})} \qquad \xi = \frac{\ell}{L}$$

$$t_{PCM} = \frac{(T_{i,h} - T_{PCM})}{(T_{i,h} - T_{i,c})} \qquad \vartheta = \psi \frac{v_f}{\epsilon_B L} \tau$$

and $t_{PCM}|_1$ represents the dimensionless temperature at the surface of the PCM sphere. The dimensionless groups are

$$Pe_a = \frac{L v_f \rho_f C_{p,f}}{k_{ef}} \qquad St = \frac{3(1-\epsilon_B) h_B L}{R_{PCM} v_f \rho_f C_{p,f}}$$

where the fluid effective thermal conductivity, k_{ef}, is given by

$$k_{ef} = \frac{k_f \epsilon_B}{\tau_B}$$

The forcing function is defined as

$$t^i = \begin{cases} 1 & \text{for heating period} \\ 0 & \text{for cooling period} \end{cases} \tag{3.8}$$

In general, the Danckwerts BCs apply:

$$\xi = 0\,; \qquad t_f - \frac{1}{Pe_a} \frac{\partial t_f}{\partial \xi} = t^i \tag{3.9.a}$$

$$\xi = 1\,; \qquad \frac{\partial t_f}{\partial \xi} = 0 \tag{3.9.b}$$

For long regenerators the Hulburt BCs may be used:

$$\xi = 0\,; \qquad t_f = t^i \tag{3.9.c}$$

$$\xi \to 1\,; \qquad \frac{\partial t_f}{\partial \xi} \to 0 \tag{3.9.d}$$

When modeling a PCR cycle, the IC is given by the final condition of the previous period, *i.e.* for the x period

$$\text{for a cocurrent PCR} \qquad t_f(0,\xi) = t_f^p(\theta_{1-x}, \xi) \tag{3.10.a}$$

$$\text{for a countercurrent PCR} \qquad t_f(0,\xi) = t_f^p(\theta_{1-x}, 1-\xi) \tag{3.10.b}$$

where $t_f^p(\vartheta,\xi)$ represents the dimensionless temperature profile at time $\vartheta = \theta_{1-x}$ for the previous period, and $1-x$ represents the subscript for the previous period (*e.g.* if $x = h$ then $1-x = c$). The IC for a single blow is obtained by replacing t_f^p with t^i.

3.3.2. PCM Scale Description

Either front-tracking or fixed-domain methods can be applied to solve the Stefan problem. Both will be described here.

3.3.2.1. Front-Tracking Method. In the front-tracking method eq. 2.9 subject to the BCs 2.10 and 2.11.a to 2.11.c is solved. Supplementing previous nomenclature, define:

dimensionless y phase temperature $(\cdot)$	t_y
dimensionless radius $(\cdot)$	φ
y-phase dimensionless inner radius in x period $(\cdot)$	$\omega_{x,y,i}$
y-phase dimensionless outer radius in x period $(\cdot)$	$\omega_{x,y,o}$
s/l-interface dimensionless radius $(\cdot)$	δ_d
Biot number $(\cdot)$	Bi

The nondimensionalized PDEs are represented by

$$\frac{1}{\varphi^2}\frac{\partial}{\partial\varphi}\left(\varphi^2\frac{\partial t_y}{\partial\varphi}\right) = \frac{3\,Bi}{St}\frac{\partial t_l}{\partial\vartheta}\ ; \qquad \omega_{x,y,i} < \varphi < \omega_{x,y,o} \tag{3.11}$$

where

$$\omega_{h,s,i} = 0 \qquad \omega_{h,s,o} = \delta_d \qquad \omega_{h,l,i} = \delta_d \qquad \omega_{h,l,o} = 1$$

$$\omega_{c,l,i} = 0 \qquad \omega_{c,l,o} = \delta_d \qquad \omega_{c,s,i} = \delta_d \qquad \omega_{c,s,o} = 1$$

with

$$\varphi = \frac{r}{R_{PCM}} \qquad\qquad \delta_d = \frac{\delta}{R_{PCM}}$$

The position of the solid/liquid interface given by δ_d is obtained by an energy-flux balance

$$\frac{\partial t_s}{\partial \varphi} - \frac{\partial t_l}{\partial \varphi} = \frac{3\,Bi}{St\,Ste}\,\frac{\rho_{PC}}{\rho_{PCM}}\,\frac{d\delta_d}{d\vartheta} \;; \qquad \varphi = \delta_d \tag{3.12}$$

The Biot number is defined as

$$Bi = \frac{h_B R_{PCM}}{k_{PCM}}$$

The BCs to be applied to eq. 3.11 are

$$\varphi = 0 \;; \qquad \frac{\partial t_{yi}}{\partial \varphi} = 0 \tag{3.13.a}$$

$$\varphi = \delta_d \;; \qquad t_s = t_l = t_M \tag{3.13.b}$$

$$\varphi = 1 \;; \qquad \frac{\partial t_{yo}}{\partial \varphi} = Bi(t_f - t_{yo}) \tag{3.13.c}$$

where

for a heating period	$yi = s$	$yo = l$
for a cooling period	$yi = l$	$yo = s$

Note

$$t_{PCM} = t_{yo}\Big|_{\varphi=1}$$

The IC for the PCM scale is

$$\vartheta = 0 \;; \qquad 0 \le \varphi \le 1 \;; \qquad t_{yo} = t_M \tag{3.14}$$

Equation 3.11 assumes constant and equal physical properties for the solid and liquid phases per assumption 3. Further, by assumption 4 there is only one interface during phase change. In addition, as discussed in Chapter 2, the phase-change component conductivity must be of the same order of magnitude or greater than the support-matrix conductivity for eq. 3.11 to be valid. If this is not true, a fixed-domain approach must be implemented.

3.3.2.2. Fixed-Domain Method. Alternatively, the PCM scale can be modeled using the enthalpy method. The dimensionless enthalpy function, u, is

$$u = t_{PCM} + \chi\, Ste \tag{3.15}$$

which has been derived from eq. 2.13 assuming $C_{p,PCM}$ is constant. The temperature within the PCM sphere is now given by the modified conduction equation:

$$\frac{\partial u}{\partial \vartheta} = \frac{3\,St}{Bi}\,\frac{1}{\varphi^2}\,\frac{\partial}{\partial \varphi}\left(\varphi^2\,\frac{\partial t_{PCM}}{\partial \varphi}\right) \tag{3.16}$$

The BCs are

$$\varphi = 0\,; \qquad \frac{\partial t_{PCM}}{\partial \varphi} = 0 \tag{3.17.a}$$

$$\varphi = 1\,; \qquad \frac{\partial t_{PCM}}{\partial \varphi} = Bi\,(t_f - t_{PCM}) \tag{3.17.b}$$

The IC is

$$\vartheta = 0\,; \qquad 0 \le \varphi \le 1\,; \qquad t_{PCM}(0,\varphi) = t^{p}_{PCM}(\theta_{1-x},\varphi) \tag{3.18}$$

where again the superscript p and the subscript $1-x$ denote the profile from the previous period.

Two sets of model equations for the PCR can be formulated. One set is formed from the ADE 3.7 coupled with the two PDEs represented by eq. 3.11 and the ordinary differential equation (ODE) for the solid/liquid interface, eq. 3.12. The other set is formed from the ADE coupled with one PDE 3.16 and the definition of the enthalpy function, eq. 3.15.

This concludes the presentation of preliminary work. Then next chapter outlines a research plan for achieving the objectives of this proposal.

4. Proposed Work

This final chapter is subdivided into four sections. The first section outlines an action plan for meeting the first objective: *viz.* developing models for single-blow PCRs. The second section presents a plan for achieving the second objective: modeling cyclic operation of PCRs. The third section presents an outline for reaching the third objective: experimental verification of the models. The final section presents a timetable for all proposed work.

4.1. Single-Blow Models

The model equations presented in Chapter 3 can be numerically solved by a variety of techniques. The models are based upon three independent coordinates: two spatial – the bed and the PCM, and one temporal. Discretization of one or more of the coordinates allows one to integrate along the remaining coordinate(s). Since the spatial coordinates span an *a priori* known domain, *viz.* $[0,1]$, discretization in space and integration along time, the method of lines, is a simple and often effective approach.

Regardless of how the Stefan problem is treated, the ADE must be discretized. Approaches such as collocation [46], collocation on finite elements [47] , finite elements and finite differences are applicable. For large values of Pe_a Deans and Lapidus [48] have shown that a central finite differences representation of the ADE is equivalent to the tanks-in-series representation of dispersion; thus the PDE is reduced to N (where $N = Pe_a/2$) ODEs. The PCR is modeled as N mixing cells.

The finite differences approach may be used even when Pe_a is too small to justify the tanks-in-series representation: gradients in space are converted to linear

differences of t_f at discretized ξ. In this case a compartments representation (see Wen and Fan [49]) is produced. This representation again can be assigned an analogy to well-stirred cells which are interconnected to account for forward and backward mixing.

If the fluid in the PCR is a gas the accumulation parameter, ψ, is generally very small ($\psi < 10^{-3}$). In this case the pseudo steady-state approximation may be invoked and the ADE may be further simplified to a set of N nonlinear equations.

The front-tracking formulation represented by eq. 3.11 can be discretized in space to convert the PDEs into ODEs. If the Stefan number is small (*e.g.* $Ste < 10^{-2}$) the pseudo steady-state assumption may be invoked on the PCM-sphere scale, converting the PDEs of eq. 3.11 into ODEs which can be analytically integrated. Then eq. 3.12 applied in each of the N cells would be integrated along with the tanks-in-series equations.

Another approximation which can be made is to assume that the liquid phase convection is so strong that this phase is completely mixed. In this case the temperature gradient $\partial t_l / \partial \varphi$ is zero; the temperature throughout the liquid phase must be t_M. The Stefan problem is reduced to a single-phase problem, *i.e.* the conduction problem need only be solved for the solid phase. The solid-phase spatial gradient can be handled by collocation methods. This approximation may be valid for a encapsulated PCM, but not for a supported PCM. Of course melt convection can be handled as described by Moore *et al.* [39], but the coupling of this model with the bed-scale description may be problematical.

With the front-tracking formulation one must account for sensible heat storage independently of phase-change heat storage. One technique for handling this is invoking Duhamel's Theorem [25]. For each mixing cell the temperature history while the PCM is a single phase is recorded. The convolution of the fluid temperature and a homogeneous solution to the conduction problem gives $t_{PCM}|_1$ required in the ADE or mixing-cell representation. The convolution integral may

be analytically evaluated assuming the fluid temperature is given by a cubic polynomial in time. The evaluation of $t_{PCM}|_1$ would then require fitting the history to cubic splines. Then $t_{PCM}|_1$ is obtained by substitution of the spline coefficients into the integrated expression.

The fixed-domain representation is more elegant since sensible heat storage is automatically included. A finite difference representation of the problem as described by Shamsundar and Sparrow [32] could be employed in this problem; however, instead of discretizing both temporally and spatially, one would discretize in space. On the PCM scale there would be M ODEs for each mixing cell. $N \times M$ ODEs would be integrated.

After both representations are programmed on the computer (for both gas and liquid PCR fluid) comparisons can be made between computational efforts, speed, and accuracy. Thermal efficiency can be obtained by quadrature and investigated as a function of dimensionless groups.

4.2. Modeling of Cyclic PCRs

Once computer models for single-blow operation are developed the open method of establishing cyclic equilibrium that was described in Chapter 2 may be used: the computer programs repeatedly solve the equations, cycling between hot and cold periods until the steady cycle is obtained. This procedure could be complicated with the front-tracking formulation since there may be a possibility of multiple solid/liquid interfaces if the PCR is cycled at high frequency. In addition, the temperature histories and interface positions, δ for each of the N cells, must be accounted for and rearranged when the PCR is swung.

Finding the equilibrium cycle by closed methods is more elegant. The front-tracking formulation can be used only in the approximation of no sensible heat storage. This is not practical.

A closed method approach may be attempted on the fixed-domain formulation. The discretized model consists of $M \times N$ ODEs which are linear in the $M \times N$ unknowns. Laplace transformation of the ODEs reduces the system to a set of equations. These equations are forced with a periodic function which can be represented in the Laplace domain. The equilibrium cycle is obtained by application of frequency response techniques.

Alternatively, the equations can be discretized in time as well as space. If there are O time steps there are $N \times M \times O$ equations that can be solved for the equilibrium cycle by equating one cycle to the next. The time discretization is devised so that O steps give exactly one cycle. If the step sizes are small a very large number of equations must be handled. If these equations are linear this does not pose a problem; however if they are nonlinear some linearization may be required.

Once the equilibrium cycle is found the overall efficiency can be calculated. Since it is expected the PCRs will operate with $t_M \neq 0.5$ the problem of scheduling units will need to be addressed. Analysis of the equilibrium cycle as a function of dimensionless groups will provide some insight into proper scheduling.

A key question in this analysis is how does the discretization affect the calculation of the equilibrium cycle, *i.e.* is the cycle calculated in this way the true equilibrium cycle, or does discretization introduce errors? Some effort must be made in ascertaining the answer to this question.

4.3. Experimental Verification

Experiments aimed at verifying the models developed are planned. A major task in this portion of the project is fabrication of the PCM spheres. One method would be to use a porous sphere which can retain the liquid phase by capillary forces. Such a concept was proposed by Olszewski [42] for high temperature

heat storage. Shell International Chemical Company, Ltd. manufactures a high porosity catalyst carrier which may be used. The product, Shell S-980-A, is a 3 mm dia. silica sphere with a porosity of 0.7. These spheres could be filled with 1-octadecane parafin which melts at a manageable temperature of 301.2 °K. The average pore diameter is 15 nm; the capillary pressure generated by a parafin (surface tension of 27.45 μN/m) in this pore is 7.3 kPa. The ratio of latent heat to sensible heat is $73/\Delta T$; thus in an experiment where the temperature rise is 5 °K, fifteen times more heat is stored in the phase change than in the sensible heating of the parafin and silica. The thermal conductivity of the silica matrix is approximately five times that of the wax, so the heat conduction in the PCM matrix will actually be higher than it would be in the solid wax phase. To properly model this system the effective thermal conductivity of the PCM, k_{PCM} , will have to be modified to include enhanced heat conduction. The silica-supported PCM would be stable in a gas environment; but may be unstable in many liquids because either the wax will be dissolved by the liquid, or the wax will be displaced by the liquid.

One attractive feature of this system is the visual indication of the phase: the solid is opaque, while the liquid is perfectly transparent. One may observe the movement of the melt front within the sphere, or more apropos, within the bed. Because of the small pore diameter there is no melt convection, with the exception of the small flow which may be produced because of solid/liquid density differences.

Another candidate PCM could be an inert-shell encapsulated wax. Fabrication of microencapsulated octadecane and eicosane has been reported [38]; however the diameter of these spheres (50 to 100 μm) is outside the target range of 3 mm to 7 mm dia. that is anticipated for these experiments. Some exploratory effort at fabricating encapsulated PCM should be made. If this effort is fruitful, this material could be used in model evaluation.

An alternative to conventional encapsulation would be to fill hollow spheres with a PCM. Hollow 70/30 brass (or aluminum) spheres used in making bead chain are available. The diameters of these spheres range from 2.4 mm to 9.5 mm. Because of the method of fabrication, *viz.* spinning/swaging, the wall thickness of the shell occupies 35 percent of the sphere volume. For the brass/octadecane system the ratio of latent heat to sensible heat is $54/\Delta T$. The beads have holes at the poles of the sphere. The diameter of these hole range from 1.1 mm for the smallest sphere to 2.0 mm for the largest. Once the sphere is filled, the holes can be sealed with solder or some organic adhesive/filler (*e.g.* epoxy, silicone, *etc.*). The high thermal conductivity of the metal would increase the axial conduction of heat along the length of the bed. Unless a simple method for easily sealing the holes is found, however, this alternative does not seem practical since about 5000 to 15000 of these spheres are required.

Besides these metal spheres, hollow plastic spheres are available. The smallest spheres are 10 mm in diameter and made of polypropylene or polyethylene. Estimates of wall thicknesses were not available from the manufacturer, but it is believed these spheres have a 0.5 mm thick wall. The spheres would have to be filled by a syringe. The puncture could be sealed by melting the plastic over the puncture. Unless a method for automating the filling process is found this is not practical.

Once the PCM is manufactured a PCR would be constructed. Figure 4.1 shows a sketch of the proposed apparatus. A transparent plexiglass column approximately 5 to 10 cm in diameter and 50 to 75 cm long would contain the PCM. The PCR is insulated by a vacuum jacket contained by a concentric outer tube of transparent plexiglass. O-rings pressed against flanges would seal the vacuum jacket, yet permit convenient disassembly of the unit. Flange fasteners may not be necessary since atmospheric pressure against the flange faces will compress the o-rings. Thermocouples positioned inside the column measure the temper-

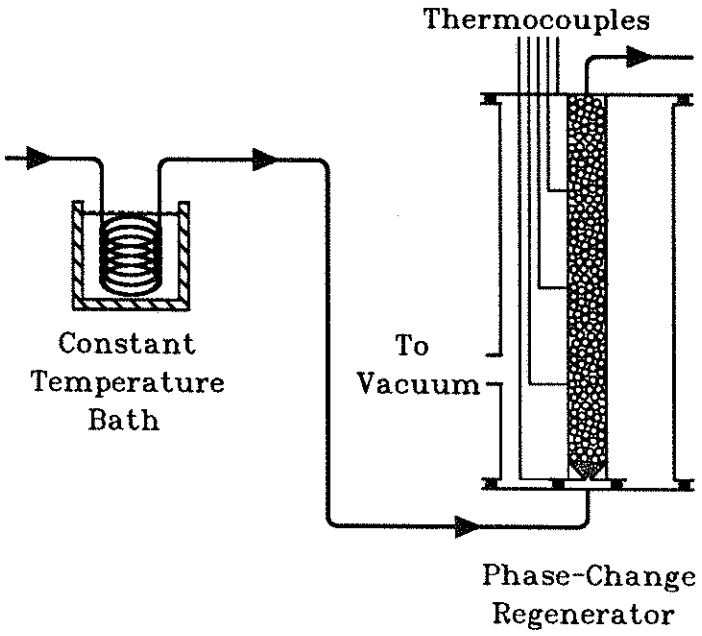

Figure 4.1 Sketch of experimental apparatus.

ature profile. A data acquisition computer will be used to read and store this information.

The fluid is introduced at the bottom of the column and distributed by a low heat capacity distributor: either hollow glass beads, or the S-980-A beads. Fluid is maintained at a constant temperature by flowing it through coils immersed in a constant temperature bath. In the case of cycling regenerators, two constant temperature baths are used and a valve selects the temperature of the PCR inlet fluid. For experiments in countercurrent cycling an additional distributor must be positioned at the top of the PCR.

Data acquired during the experiment consists of temperature profiles and fluid outlet temperature. In addition, phase change may be observed if the PCM undergoes a transition from opaque to transparent; the front position as a function of time can be recorded in this case.

At this point the optimal PCM can be selected. The working model describing

this material will be established. Comparison between the model and experimental data can then be made. Both temperature profiles and thermal efficiencies can be calculated. The experimental PCR equilibrium cycle can be compared against the calculated cycle.

4.4. Timing

It is planned this research will be completed by the end of the year. Table 4.1 presents estimates for the time required to complete the work.

Table 4.1
Timetable for research

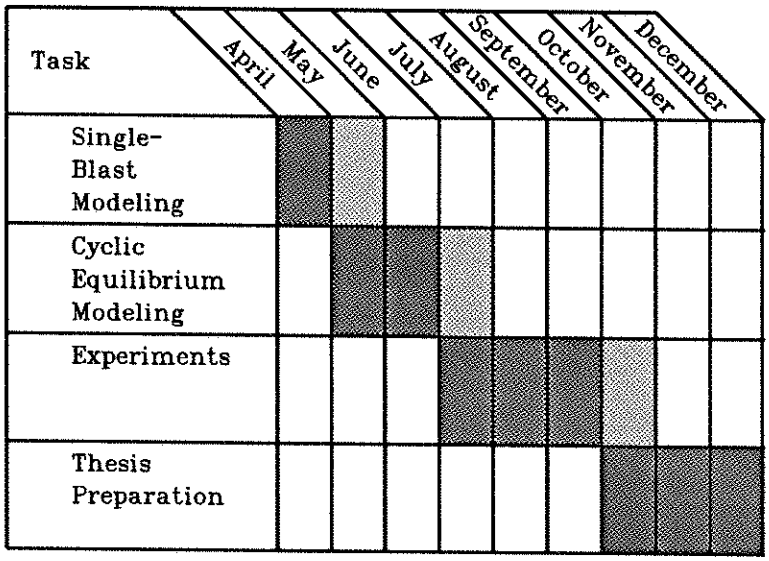

This concludes the presentation of proposed work.

5. Nomenclature

Acronyms

ADE	Axial Dispersion Equation
PC	Phase-change Component
PCM	Phase-Change Materials
PCR	Phase-Change Regenerator
SC	Support-matrix Component

Symbols

Bi	Biot number; p. 36
C_p	heat capacity, J/kg °K
h	convective heat transfer coefficient, W/m^2 °K
k	thermal conductivity, W/m °K
L	regenerator length, m
ℓ	regenerator axial length coordinate, m
$\dot{m}$	fluid mass flowrate, kg/s
N	number of mixing cells
Pe	Peclet number for heat transfer; p. 34
Q	heat energy, J
R	maximum radius, m
r	spherical coordinate, m
St	Stanton number for heat transfer; p. 34
Ste	Stefan number; p. 26
T	temperature, °K
t	dimensionless temperature; eq. 2.5
U	enthalpy function, J/kg; eq. 2.13
u	enthalpy function; eq. 3.15
v	fluid superficial velocity, m/s

Greek Symbols

δ	melt front coordinate, m
ϵ	porosity, m^3/m^3
φ	sphere coordinate; p. 35
η	efficiency; eq. 2.3
κ	period fraction; eq. 3.6
λ	latent heat of fusion, J/kg
μ	temperature break-though time; p. 26
χ	melt fraction; p. 21

ρ	density, m^3/kg
τ	time coordinate, s
$\mathcal{T}$	tortuosity, m/m
θ	regenerator period, s
ϑ	time coordinate; p. 34
ψ	accumulation parameter; p. 26
ω	domain endpoint; p. 35
ξ	regenerator axial coordinate; p. 34

Subscripts[†]

a	axial
B	bed
c	cooling period
d	dimensionless
f	fluid
h	heating period
i	inlet [first][‡]; inner [third]
l	liquid phase
M	melting point
o	outlet [first]; outer [third]
PC	phase-change component
PCM	PCM (effective) property
PCR	PCR (regenerator) property
p	packing (for C_p apply to [second] only)
SC	support-matrix component
s	solid phase
x	generic for h and c
y	generic for s and l
yi	generic for inner phase s or l
yo	generic for outer phase s or l
z	generic for SC or PC
$1-x$	opposite of x

Superscripts

i	initial
id	ideal
o	overall
p	previous

[†]Multiple subscripts are separated by commas.

[‡]Brackets designate the position of the subscript.

6. Bibliography

[1] Gunn, Marvin E., "Recovery of Industrial Waste Heat", in *Utilization of Reject Heat*, ch 2, Mitchell Olszewski, editor, Marcel Dekker, Inc., New York, 1980.

[2] Hunt, V. Daniel, *Handbook of Conservation of Solar Energy, Trends and Perspectives*, ch 2, Van Nostrand Reinhold Company, New York, 1982.

[3] Lane, George A., *Solar Heat Storage: Latent Heat Materials. Volume I: Background and Scientific Principles*, ch 1, CRC Press, Boca Raton, Florida.

[4] Reiter, Sydney, *Industrial and Commercial Heat Recovery Systems*, ch 4, Van Nostrand Reinhold Company, Inc., Cincinnati, 1983.

[5] Reay, D. A., *Heat Recovery Systems – A directory of equipment and techniques*, Halsted Press, New York, 1979.

[6] Hausen, Helmuth, *Heat Transfer in Counterflow, Parallel Flow and Cross Flow*, chs 11-19, translated from German by M. S. Sayer, edited by A. J. Willmott, McGraw-Hill, Inc., New York, 1983.

[7] Davies, Mansel, *The Physical Principles of Gas Liquefaction and Low Temperature Rectification*, pp. 93-109 and pp. 125-134, Longmans, Green and Co., London, England 1949.

[8] Schmidt, F. W. and A. J. Willmott, *Thermal Energy Storage and Regeneration*, Hemisphere Publishing Corporation, New York, 1981.

[9] Levenspiel, Octave, *Chemical Reaction Engineering*, Second edition, ch 9, John Wiley & Sons, Inc., New York, 1972.

[10] Jakob, Max, *Heat Transfer, Volume II*, ch 35, John Wiley & Sons, Inc., New York, 1957.

[11] Nusselt, W., "Die Theorie des Winderhitzers," *Z. Ver. deut. Ing.* **71**, 85 (1927).

[12] Anzelius, A., "Über Erwärmung vermittels durchströmender Medien," *Z. Angew. Math. Mech.* **6**, 291 (1926).

[13] Schumann, T. E. W., "Heat Transfer: A Liquid Flowing Through a Porous Prism," *J. Franklin Inst.* **208**, 405 (1929).

[14] Klinkenberg, A., "Heat Transfer in Cross-Flow: Heat Exchangers and Packed Beds," *Ind. Eng. Chem.* **46**, 2285 (1954).

[15] Larsen, Floyd W., "Rapid Calculation of Temperature in a Regenerative Heat Exchanger Having Arbitrary Initial Solid and Entering Fluid Temperatures," *Int. J. Heat Mass Transfer* **10**, 149 (1967).

[16] Handley, D. and P. J. Heggs, "The Effect of Thermal Conductivity of the Packing Material on Transient Heat Transfer in a Fixed Bed," *Int. J. Heat Mass Transfer* **12**, 549 (1969).

[17] Schmidt, F. W. and J. Szego, "Transient Response of a Hollow Cylindrical-Cross-Section Solid Sensible Heat: Storage Unit – Single Fluid," and "Analysis of the Effects of Finite Conductivity in the Single Blow Heat Storage Unit," *J. Heat Transfer* **100**, 737 and 740 (1978).

[18] Burch, D. M., R. W. Allen and B. A. Peavy, "Transient Temperature Distributions Within Porous Slabs Subjected to Sudden Transpiration Heating," *J. Heat Transfer* **98**, 221 (1976).

[19] Lai, Shin-Ming, *Periodic Operation of Heat Regenerators: A New Method for Calculation of Thermal Efficiency*, Master of Science Dissertation, Washington University, St. Louis, Missouri, 1983.

[20] Lu, P. -C., "Single-Blow Transients in Packed-Bed Storage Units With Solid-Phase Conduction by Crump's Numerical Inversion of Laplace Transforms," *J. Heat Transfer* **105**, 493 (1983).

[21] Ackermann, G., "Die Theorie der Wärmeaustauscher mit Wärmespeicherung," *Z. Angew Math. Mech.* **11**, 192 (1931).

[22] Nahavandi, A. N. and A. S. Weinstein, "A Solution to the Periodic-Flow Regenerative Heat Exchanger Problem," *Appl. sci. Res.* **10**, 335 (1961).

[23] Kardas, Alan, "On a Problem in the Theory of the Unidirectional Regenerator," *Int. J. Heat Mass Transfer* **9**, 567 (1966).

[24] Willmott, A. J., "The Regenerative Heat Exchanger Computer Representation," *Int. J. Heat Mass Transfer* **12**, 997 (1969).

[25] Carslaw, H. S. and J. C. Jaeger, *Conduction of Heat in Solids*, Second Edition, pp 30-33, pp 240-241, ch XI, Oxford University Press, Great Britain, 1959.

[26] Crank, John, *Free and moving boundary problem*, chs 3-6, Clarendon Press, Oxford, 1984.

[27] Muehlbauer, John C. and J. Edward Sunderland, "Heat Conduction with Freezing or Melting," *Appl. Mech. Rev.* **18**, 951 (1965).

[28] Mori, A. and K. Araki, "Methods for analysis of the moving boundary-surface problem," *Int. Chem. Eng.* **16**, 734 (1976).

[29] Furzeland, R. M., "A Comparative Study of Numerical Methods for Moving Boundary Problems," *J. Inst. Maths. Applics.* **26**, 419 (1980).

[30] Schneider, G. E. and M. J. Raw, "An Implicit Solution Procedure for Finite Difference Modeling of the Stefan Problem," *AIAA J.* **22**, 1685 (1984).

[31] Chawla, T. C., D. R. Paddersen, G. Leaf, W.J. Minkowycz and A. R. Shoumann, "Adaptive Collocation Methods for Simultaneous Heat and Mass Diffusion With Phase Change," *J. Heat Transfer* **106**, 491 (1984).

[32] Shamsundar, N. and E. M. Sparrow, "Analysis of Multidimensional Conduction Phase Change Via the Enthalpy Model," *J. Heat Transfer* **97**, 333 (1975).

[33] Cambell, S., in *Energy Utilization: A Sourcebook of Current Technology*, ch 56, The Fairmont Press, Inc., Atlanta Georgia, 1980.

[34] Katayama, K., Akio Saito, Yoshio Utaka, Akihiro Saito, Hideo Matsui, Hiromichi Maekawa, and A. Z. A. Saifullah, "Heat Transfer Characteristics of the Latent Heat Thermal Energy Storage Capsule," *Solar Energy* **27**, 91 (1981).

[35] Rieger, H., U. Projahn, M. Bareiss, H. Beer, "Heat Transfer During Melting Inside a Horizontal Tube," *J. Heat Transfer* **105**, 226 (1983).

[36] El-Masry, Said El-Sayed, "Numerical Investigation of Phase Change Heat Transfer in a Horizontal Cylinder Including Effects on Natural Convection," Ph. D. dissertation, University of Miami, Coral Gables, Florida, May, 1984.

[37] Mulligan, J. C., "Phase-Change Heat-Storage Module," *NASA Tech Briefs* **13**, 103 (1989).

[38] NASA Technical Support Package MFS-26071, "Phase-Change Heat-Storage Module," available through NASA Scientific and Technical Information Facility, Washington D. C. (1989).

[39] Moore, F. E. and Y. Bayazitoglu, "Melting Within a Spherical Enclosure," *J. Heat Transfer* **104**, 19 (1982).

[40] Morrison, D. J. and S. I. Abdel-Khalik, "Effects of Phase-Change Energy Storage on the Performance of Air-Based and Liquid-Based Solar Heating Systems," *Solar Energy* **20**, 57 (1978).

[41] Bliem, C., D. J. Landini, J. F. Whitbeck, R. Kochan, J. C. Mittl, R. Piscitella, J. Schafer, A. Synder, D. J. Wiggins, J. M. Zabriskie, B. A. Barna, S. P. Henslee, P. V. Kelsey, J. I. Federer and E. S. Bomar, *Ceramic Heat Exchanger Concepts and Materials Technology*, pp. 33-38, pp. 153-154 and pp. 171-199, Noyes Publications, Park Ridge, New Jersey, 1985.

[42] Olszewski, M., "Advanced Latent Heat Storage Media for High-Temperature Industrial Applications," NTIS, document no. DE 85000907, 1984.

[43] Arimilli, Rao V., "Modeling of Transient Heat Transfer in Packed Beds," in *Proceedings of the U. S. D. O. E. Thermal Energy Storage Program Review: Report to Industry*, March 11-12, 1987.

[44] Adebiyi, Geaoge A., "Development of PCM Packed Bed Thermal Model for Industrial Applications," in *Proceedings of the Diurnal/Industrial Thermal Energy Storage Research Activities Review*, March 9-10, 1988.

[45] Larkin, Bert K. and Stuart W. Churchill, "Heat Transfer by Radiation through Porous Insulations, " *A.I.Ch.E. J.* **5**, 467 (1959).

[46] Villadsen, John and Michael L. Michelsen, *Solution of Differential Equation Models by Polynomial Approximation*, chs 3-4 and 8-9, Prentice-Hall, Inc., Englewood Cliffs, New Jersey, 1978.

[47] Madsen, N. K. and R. F. Sincovec, "ALGORITHM 540 PDECOL, General Collocation Software for Partial Differential Equations [D3], " *ACM Trans. Math. Soft.* **5**, 326 (1979).

[48] Deans, H. A. and Leon Lapidus, "A Computational Model For Predicting and Correlating the Behavior of Fixed-Bed Reactors: I. Derivation of Models for Nonreacting Systems," *A.I.Ch.E. J.* **6**, 656 (1960).

[49] Wen, C. Y. and L. T. Fan, *Models for Flow Systems and Chemical Reactors*, ch 7, Marcel Dekker, New York, 1975.